The Effect of Over Expression of Human Cystathionine beta Synthase (hCBS) on the Level of Glutathione in Mammalian Cells: A Model System for the Study of the Effect of Naturally Occurring Missense Mutations of hCBS on Glutathione

By

Muluken S. Belew, B. Sc. (Great Distinction)

A thesis submitted to

The Faculty of Graduate Studies and Research

in partial fulfillment of

the requirements of the degree of

Master of Science

Biology Department

Ottawa-Carleton Institute of Biology

Carleton University

Ottawa, Ontario

April 2008

Your file Votre référence
ISBN: 978-0-494-40653-3
Our file Notre référence
ISBN: 978-0-494-40653-3

ABSTRACT

L-Cysteine is the biosynthetic precursor for a number of compounds, including the large intracellular store of the antioxidant, glutathione. It has been observed that more than 50% of the L-Cys required for the synthesis of glutathione is produced *via* the transsulfuration pathway. Human cystathionine β-synthase (hCBS) catalyzes the first and committing step in the transulfuration pathway. There are more than 100 naturally-occurring missense mutations affecting the catalytic activity of this enzyme. Transfection of COS7 cells with select, naturally-occurring mutants of hCBS was conducted to investigate their effect on the level of glutathione, as compared to the wildtype enzyme. It was noted that the transfectants expressing wild-type CBS showed nearly 35% increase in the level of total glutathione. This contrasts with the G307S, G305R, G259S, G148R, and I278T mutants, which had negligible effect on the cellular glutathione concentration. The conventional enzymatic method of glutathione determination was modified, to increase its range and sensitivity, as an important initial step in this study. The steady state kinetic parameters of the hCBS mutants selected were determined (whenever possible) in order to explain the possible mechanism by which cellular glutathione levels are regulated by this enzyme. Such *in vitro* studies on the enzyme require sufficiently pure form of the enzyme. Therefore, a novel bacterial expression system, incorporating a N-terminal 6-His tag was developed and found to be effective for the purification of hCBS *via* metal ion affinity chromatography. The $k_{cat}/k_m^{L\text{-}Hcys}$ and $k_{cat}/k_m^{L\text{-}Ser}$ of the 6-His-tagged enzyme is almost ten- and two-fold greater respectively than the conventionally-expressed enzyme. This expression system is used to purify the wildtype and select mutants of the enzyme.

ACKNOWLEDGMENT

First and foremost, I would like to express my heartiest thankfulness to the almighty Trinity and his holy mother, St. Mary, with out whose guidance and care all the way through, I could not have possibly reached today!

Second, my deepest appreciation and gratitude goes to my supervisors, Drs. Bill Willmore and Susan Aitken who guided me all the way from my very arrival to Ottawa through my project up to now. I am really indebted to Bill and Sue for your brotherly and sisterly treatments especially at times of discouragement. You have unforgettable memories in my mind for your efforts to make me feel at home as an international student challenged by cultural shock. Your teachings and advice are stamped in my heart and will guide me all the way throughout my career. You are not just supervisors to me! Also I am grateful to Dr. Marc Ekker for being in my advisory committee and for his invaluable suggestions and remarkable ideas in my project.

Third, for all my colleagues and friends in Willmore and Aitken labs who are also part of the process of the making of this thesis come to reality; especially Pratik Lodha who shared me his skill of experimental set up of enzyme kinetics and subsequent Excel data analysis. I appreciate all the help and friendliness.

Next my warmest thankfulness goes to the benefactors of Indira Gandhi Memorial Fellowship whose financial award during my stay allowed me take the opportunity of advancing my professional career through participation at scientific conferences.

All of you who have touched my life in one way or another when I was in Ethiopia and all Ethiopian friends in Ottawa I would like to say to you that this thesis is the outcome of your work too. I am in great indebtedness for all your hospitality and encouragement especially at the time I needed it most.

DEDICATION

I dedicate this thesis to my beloved mom, W/ro Yiftusira Mengestie, who sacrificed her all living for the comfort of her children. Muntaye you are not just a mother!

TABLE OF CONTENTS

Chapter Two

Coupled Enzyme NADPH-Recycling Assay for Measuring Total And Oxidized Glutathione: A Comparison with Other Methods

Chapter Three

Development of an Improved System for the Expression and Purification of Recombinant Human Cystathionine β-Synthase in *E. coli.*

Chapter Four

The Effect of Overexpression and Mutation of Human Cystathionine β-Synthase on the Level of Glutathione in Mammalian Cells

LIST OF TABLES

LIST OF FIGURES

LIST OF ABBREVIATIONS

ADP	Adenosine diPhosphate
AIDS	Acquired immuno deficiency syndrome
5-ALA	5-Aminolevulinic acid
Amp	Ampicilin
ATP	Adenosine triphosphate
BP	Base pair
BSA	Bovine serum albumin
BSO	Buthionine sulfoximine
CBL	Cystathionine β-lyase
CGL	Cystathionine γ-lyase
CMV	Cytomegalovirus
DEAE	Diethyl amino ethyl
DNA	Deoxyribonucleic acid
DTNB	5, 5'-Dithio-bis (2-nitrobenzoic acid)
EC- HPLC	High performance liquid chromatography with electrochemical detection
E. coli	*Escherichia coli*
EDTA	Ethylenediamine tetracetic acid
eGFP	enhanced green fluorescent protein
HIF-1α	Hypoxia inducible factor-1α
HIV	Human immunodeficiency virus
HRP	Horse Raddish peroxidase

γ-GCS	γ-Glutamyl cysteine synthase
G6P	Glucose 6 phosphate
G6PDH	Glucose 6-phosphate dehydrogenase
GLP	Glucono Lactone phosphate
GFP	Green fluorescent protein
Glu	Glutathione
GR	Glutathione reductase
GS	Glutathione synthase
GSH	Glutathione (reduced)
GSSG	Glutathione (oxidized)
GST	Glutathione S-transferase
hCBS	human cystathionine β-synthase
HEK 293	Human embryonic kidney cell line
His	Histidine
IPTG	Isopropyl-β-D-thiogalactopyranoside
KDa	Kilodalton
KPi	Potassium phosphate
L-Cth	L-cystathionine
L-Cys	L-cysteine
LDH	Lactate dehydrogenase
L-Hcy	L-homocysteine
LoD	Limit of detection
LoQ	Limit of quantification
L-Ser	L-serine

MCS	Multiple cloning site
Met	Methionine
MS	Methionine synthase
NADH	Nictotinamide adenine dinucleotide (reduced)
$NADP^+$	Nicotinamide adenine dinucleotide phosphate (oxidized)
NADPH	Nicotinamide adenine dinucleotide phosphate (reduced)
NF-κB	Nuclear factor-κB
Ni-NTA	Nickel-nitrilo triacetic acid
PAGE	Polyacrylamide Gel Electrophoresis
PC-12AC	Rat Adrenal Pheochromocytoma -12 Adherent Clone cells
PCR	Polymerase chain reaction
PLP	Pyridoxine phosphate
SAE	S-adenosine ethionine
SAH	S-adenosine homocysteine
SAM	S-adenosine methionine
SDS	Sodium dodecyl sulphate
SSA	Sulfosalycilic acid
TNB	5'-Thionitrobenzoic acid

1. INTRODUCTION

1.1. Amino Acids

Organic molecules comprising both amino and carboxylic functional groups are referred to as amino acids. This term is commonly used in biochemistry/molecular biology to refer to α-amino acids, in which the amino and carboxylic acid are attached to the α-carbon atom, and in particular the 20 proteinogenic α-amino acids. These standard amino acids are represented by the formula $NH_2CHRCOOH$, where the R is the side chain, and occur in the 'L' conformation in proteins. Half of the 20 amino acids found in proteins are considered essential because they are not synthesized *de novo* by humans and, therefore, must be obtained from the diet (Shike, 2006). The amino acid cysteine is derived from the essential amino acid methionine, *via* the transulfuration path way, and is considered semi-essential. L-Methioine (L-Met) and L-cysteine (L-Cys), the only sulfur-containing α-amino acids are the precursors of a wide variety of metabolites, including *S*-adenosylmethionine (SAM), L-homocysteine (L-Hcys) and glutathione.

1.2. L-Homocysteine

L-Hcys is a product of the metabolism of SAM, the key cellular methyl donor. Depending on the levels L-Met within the cell, L-Hcys is either converted to L-Cys, *via* the transsulfuration pathway, or remethylated to produce L-Met, *via* the transmethylation pathway (Figure 1.1). L-Cys is the biosynthetic precursor of glutathione, the major intracellular antioxidant. It has been observed that more than 50% of the L-Cys required for the synthesis of glutathione is produced *via* the transsulfuration pathway, while the

remainder is derived from diet (Banerjee *et al.,* 2000). Therefore, L-Hcys, the branch-point between the transmethylation and transsulfuration pathways, represents the metabolic link between the methylation and redox status of the cell, as determined by the key sulphur-containing metabolites SAM and glutathione (Purdova *et al.,* 2006). The first committed step in the transsulfuration pathway is the condensation of L-Hcys and L-Ser, to form cystathionine (L-Cth), catalyzed by cystathionine β-synthase (CBS) (Medina *et al.,* 2001).

Due to its position at the metabolic branch point between L-Met and L-Cys biosynthesis, L-Hcys metabolism is tightly regulated. Flux through the competing transmethylation and transsulfuration pathways is determined by the affinities of methionine synthase (MS) and CBS, respectively, for L-Hcys. The first enzyme in the transmethylation pathway, MS has a $K_m^{L\text{-}Hcys}$ value of <0.1 mM (Chen *et al.*, 1994), considerably lower than that of hCBS ($K_m^{L\text{-}Hcys}$ = 1.04 mM) (Frank *et al.*, 2007). Therefore, at sub-millimolar L-Hcys concentrations, the flux through the transmethylation pathway exceeds that of the transsulfuration pathway due to the high affinity of MS for L-Hcys. As the cellular L-Hcys concentration increases, there is a corresponding increase in flux through the transsulfuration pathway, to produce L-Cys (Finkelstein and Martin, 1984; Finkelstein 1990). This flux is also regulated, as both MS and CBS are post-translationally regulated by SAM (Teodoro 2002).

Figure 1.1. L-Homocysteine is the metabolic link between the transsulfuration and transmethylation pathways. Abbreviations: *S*-adenosylmethionine (SAM); *S*-adenosyl homocysteine (SAH); cystathionine β-synthase (CBS); and methionine synthase (MS) (modified from Purdova *et al.*, 2006). (Figure is drawn by using ISIS^{TM} /Draw 2.4 software, MDL Information Systems Inc.)

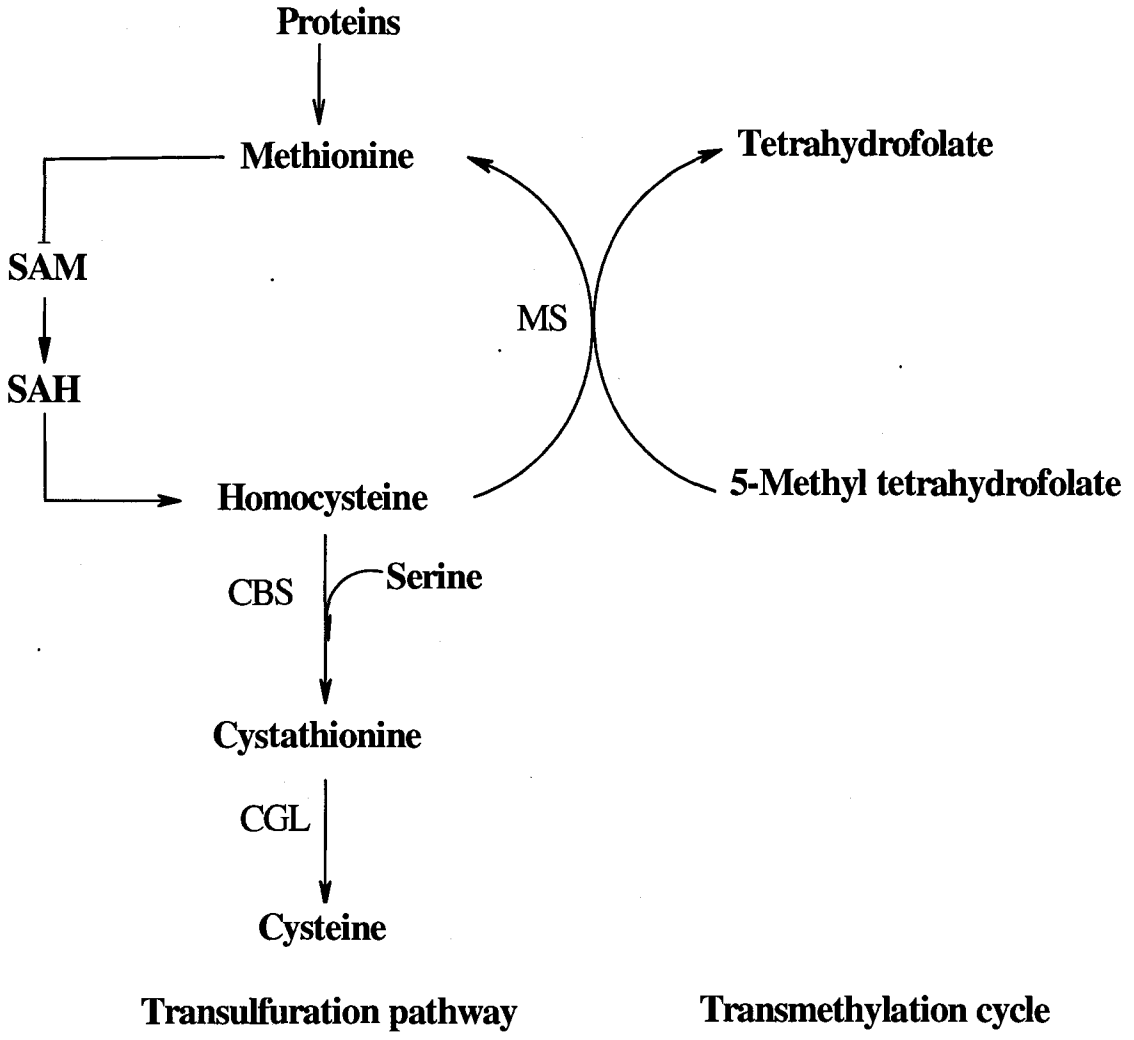
Proteins
Methionine
Tetrahydrofolate
SAM
MS
SAH
Homocysteine
5-Methyl tetrahydrofolate
CBS
Serine
Cystathionine
CGL
Cysteine
Transulfuration pathway
Transmethylation cycle

1.3. Cystathione Beta Synthase (CBS)

Human CBS (hCBS) (EC. 4.2.1.22) is a homotetrameric protein with a subunit molecular weight of 63 KDa. Each subunit comprises 551 amino acids and contains an active site, at which the catalytic cofactor pyridoxal 5'-phosphate (PLP) is covalently bound (Mudd *et al.,* 1995; Clark *et al.,* 1998). Cystathionine β-synthase from mammalian sources including hCBS, also contains a N-terminal, heme-containing domain, for which a redox-regulatory role has been proposed (Banerjee *et al.*, 1998; Meier *et al.,* 2001) (Figure 1.2). In contrast, CBS from yeast (*Saccharomyces cervisiae*) and *Trypanosoma cruzi* lack the ~70-residue, N-terminal domain and do not bind heme (Jhee *et al.,* 2000; MacLean *et al.*, 2000; Nozaki *et al.*, 2001). The PLP-containing catalytic core of CBS represents the conserved portion of the protein and resembles other members of the β-class, also known as fold-type II, of PLP-dependent enzymes (Mehta and Christen, 2000). In contrast, the evolutionary antecedence of the heme binding domain is unclear as it does not resemble other heme proteins. The reaction catalyzed by CBS is a PLP-dependent β-replacement, in which the hydroxyl group of L-Ser is replaced by thiolate group of L-Hcys, producing L-Cystathionine (L-Cth) (Figure 1.3).

Naturally occurring mutations in the gene encoding CBS, that decrease its activity or stability or modify its post-translational regulation, result in the intracellular accumulation of L-Hcys, which is exported to the extra-cellular fluid and subsequently to the blood plasma. Elevated levels of L-Hcys in the blood, a condition termed homocystinuria, is associated with a variety of clinical manifestations including mental retardation, reduced skeletal and muscle function, ectopia lentis, arteriosclerosis and other cardiovascular abnormalities (Harker *et al.,* 1974; Medina *et al.,* 2001; Kraus *et al.,* 2002).

Figure 1.2. The structure of hCBS. (**A**) Schematic representation of the modular domain structure of the hCBS protein, including the heme-binding, catalytic and regulatory domains. (**B**) Cartoon representation (PyMOL, Delano Scientific Inc., CA) of the dimeric, truncated form of hCBS, comprising the heme-binding and catalytic domains. The PLP and heme cofactors are shown in yellow and red, respectively. The PyMOL software package was employed to generate this figure (Delano Scientific Inc. CA).

A


1
67
413
551
heme-binding domain
catalytic domain
regulatory domain
N-terminus
C-terminus

B

Figure 1.3. The reactions catalyzed by CBS and cystathionine γ-lyase (CGL), which comprise the transsulfuration pathway. (Figure is drawn by using ISIS™ /Draw 2.4 software, MDL Information Systems Inc.)

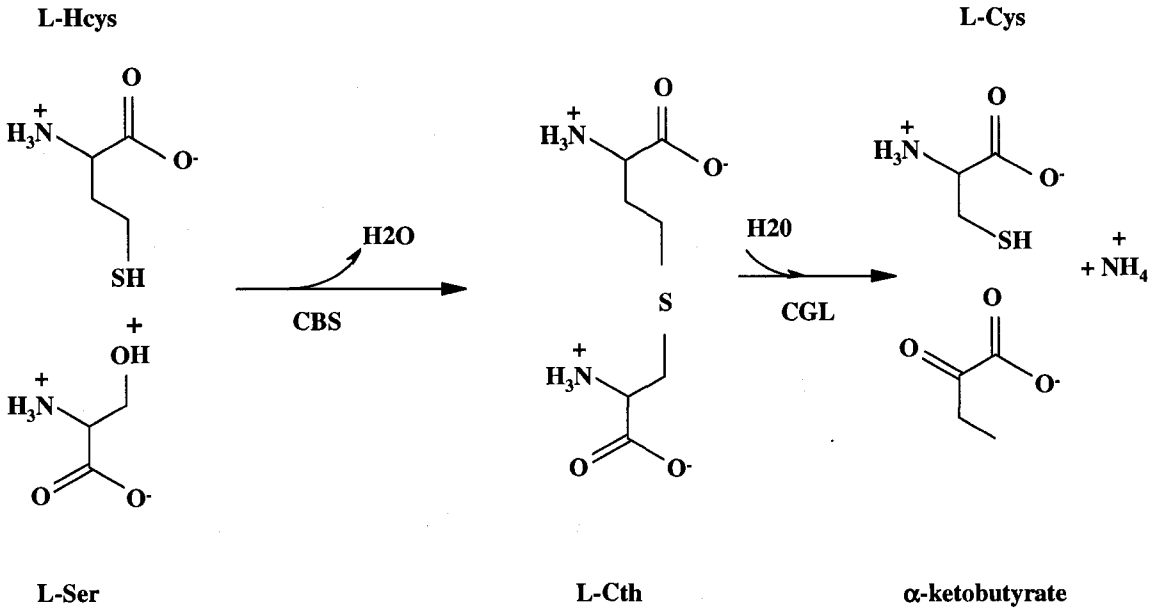
L-Hcys
L-Cys
H2O
CBS
H20
CGL
+ NH4
L-Ser
L-Cth
α-ketobutyrate

The normal concentration of L-Hcys in plasma is in the range of 5-16 μM. Plasma levels of L-Hcys in excess of this range are divided into the categories of moderate (16-30 μmol/L), intermediate (30-100 μmol/L) and severe (>100 μmol/L) homocystinuria. Patients with hyper-homocystinuria can reach plasma homocysteine values as high as 500 μmol/L (Medina *et al.*, 2001).

1.4. Location of Mutations Causing Homocystiniuria in hCBS

The more than 100 known homocystinuria-associated mutations of hCBS are distributed throughout all domains of the protein (http://www.uchsc.edu/cbs/cbsdata/mutations.htm). Analysis of the structure of the dimeric, truncated form of hCBS (amino acid residues 1-413, comprising the heme-binding and catalytic domains; Figure 1.2) demonstrates that disease-related mutations are found at the dimer interface, in the catalytic, heme binding and regulatory domains and at predicted contact regions of the regulatory domains, for which the structure is unknown (Meier *et al.*, 2003). The effect of mutations at each of these sites and corresponding pathological effects are described below.

1.4.1. Mutations at the Dimer Interface

The dimer interface of CBS is characterized by a hydrophobic area, with the amino acids Phe111 and Phe112 at the center, surrounded by polar interactions at the periphery (Meier *et al.*, 2001) (Figure 1.4). Two known mutations in this region are A114V and G116R. Residues A114 and G116 comprise a hydrophobic contact at the dimer interface. Hence, these mutations, and others in this region, may destabilize the monomer-monomer interaction. The A114V mutation is one of a large number that are at least partially rescued

by the inclusion of PLP in the assay and pyridoxine in the growth medium of the *E. coli* culture, demonstrating the dynamic nature of proteins that allows for long-range communication between and within subunits. Other point mutations which have a low frequency of occurrence observed in the dimer interface region include P78R, P88S, E176K, V180A, and R336C/H (Kraus *et al.,* 2003).

1.4.2. Mutations in the Catalytic Domain

The active site, which contains the PLP cofactor, is accessible to substrates only *via* a narrow channel. There are six known homocystinuria-associated point mutations in proximity to the activity site, which likely affect the catalytic activity of the enzyme either through inhibiting substrate binding or alteration of the binding or orientation of the PLP cofactor. Four of these mutations involve glycine residues (G148R, G305R, G307S and G259S) and the G307S is one of two most common homocystinuria-associated, pyridoxine non responsive mutations (Kraus *et al.*, 1999; Hu *et al.*, 1993) (Figure 1.5). The situation of G307 within the entry channel of the active site and the close packing of residues P282, S285 and Y301 against the side chain of this residue (Figure 1.4), may preclude substrate binding as a result of steric hindrance in the G307S mutant (Meier *et al.,* 2003).

Although the G305R mutation likely affects the binding of the PLP cofactor, as G305 contacts the *re*-face of the pyridine ring of the PLP cofactor as well as the L-Ser substrate (Meier *et al.,* 2003), patients with this mutation are responsive to pyridoxine treatment (Hu *et al.*, 1993).

Figure 1.4. Location of amino acids at the dimer interface that are the site of homocystinuria-associated mutations. Depicted is cartoon representation (PyMOL, Delano Scientific Inc., CA) of the hCBS monomer with residues of interest shown in stick representation: (**a**) R336, (**b**) F112, (c) F111, (**d**) P88, (**e**) A114, (**f**) V180 and (**g**) E176.


a
g
b
f
c
d
e

Residue G148 is situated in a stretch of amino acids that form a mobile loop, referred to as 'the asparagine loop', which interacts with the α-carboxylate group of the first substrate (corresponding to L-Ser in hCBS) in the closely-related enzyme *O*-acetyl serine sulfhydrylase (OASS) (Burkhard, *et al.,* 1999). The G148R mutation likely results in the loss of flexibility of the asparagine loop, as well as steric hindrance with the hCBS substrates. The other two mutations, G259S and T257M, the later of which is pyridoxine responsive (Meier *et al.,* 2003), affect the loop that forms extensive hydrogen bonding interactions with the phosphate moiety of the PLP cofactor, possibly altering the binding affinity of hCBS for PLP as well as the orientation of the cofactor within the active site. The pyridoxine responsiveness or non responsiveness of G259S mutations has not been reported to date.

1.4.3. Mutations in the Heme Binding Site

The heme cofactor of hCBS is located in a hydrophobic pocket and is axially coordinated by the sulfhydryl group of Cys52 and the Nε2 atom of His65 (Meier *et al.* 2001; Ojha; *et al.*, 2002). Ojha *et al.,* (2002) analyzed the spectroscopic properties of the H65R mutant of hCBS and found that, although another ligand, predicted to be H67 or P64, replaces H65 as an axial heme ligand, this mutant has reduced enzymatic activity (approximately 9 fold lower activity) and lower heme saturation (19%) than the wild type enzyme.

1.4.4. Mutations affecting Inter-Domain Communication

One of the most prevalent homocystinuria-associated mutations of hCBS is I278T, which is second only to the G307S mutant in frequency. Residue I278 is located in the middle of β-strand 9 in the β-sheet of the catalytic domain (Figure 1.6).

Figure 1.5. (**A**) Location of amino acids that are the site of homocystinuria-associated mutations within the context of the active site. View is cartoon representation (PyMOL, Delano Scientific Inc., CA) of a hCBS monomer with residues of interest shown in stick representation: (**a**) T257 and (**b**) G148, (**c**) G305, (**d**) G307 and (**e**) G259 (**B**) Amino acid residues (orange) whose side chains are in hydrophobic contact with G307 (**d**): (**f**) P282, (**g**) S285 and (**h**) Y301. The PLP cofactor is shown in yellow stick format.

A

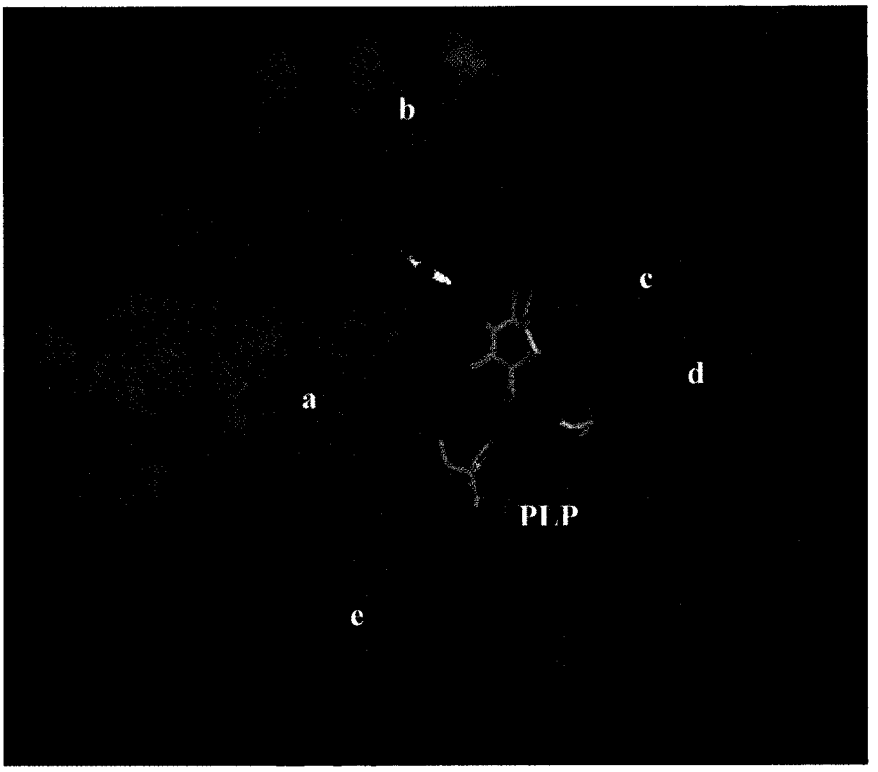

B

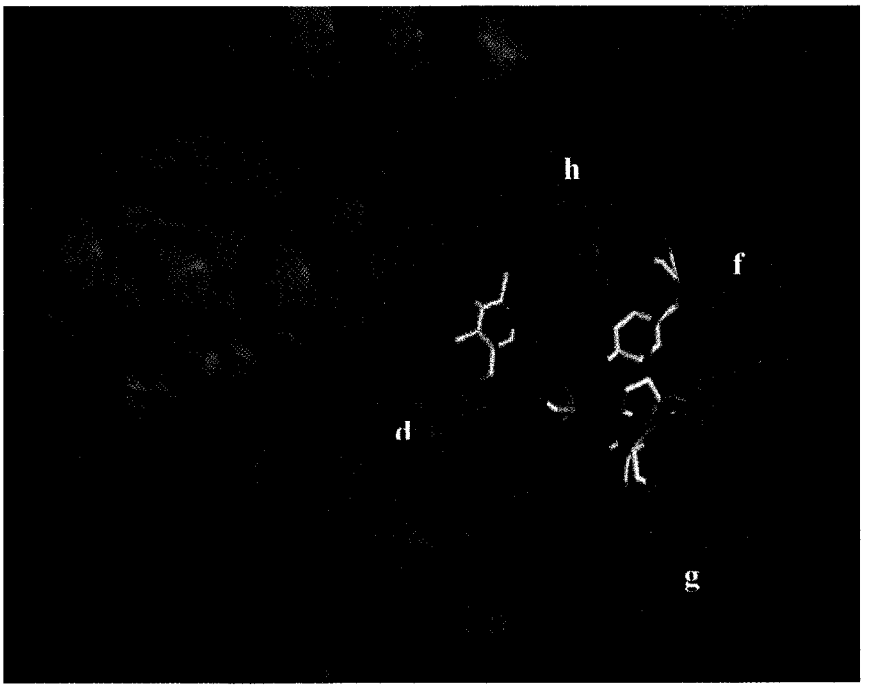

The effects of this mutation can be suppressed by mutations in the regulatory domain, suggesting that this residue is involved in communication between the regulatory and catalytic domains of hCBS (Banerjee *et al.*, 2003). Similarly, the V168M mutant, which exhibits a 7-fold decrease in PLP binding and a 13-fold decrease in activity (Banerjee and Kabil, 1999), is compensated by deletion of the C-terminal regulatory domain or specific point mutations in this region (Kruger *et al.*, 2001). These observations led Kruger *et al.* (2001) to suggest a mechanism of allosteric activation for hCBS involving the displacement of the regulatory domain from the active site.

1.5. Regulation of hCBS

1.5.1. Allosteric Regulation by SAM

The balance between conserving methionine, *via* the transmethylation pathway, under conditions of methionine restriction, and committing homocysteine to the transulfuration pathway, under conditions of methionine adequacy, is achieved *via* the post-translational regulation of MS and hCBS. Researchers have found that, under conditions of methionine restriction, hCBS activity is decreased 2-3 fold (Taoka *et al.*, 1999). Purdova *et al.* (2006) also observed that the half-life of CBS decreased during methionine restriction, suggesting that the binding of SAM stabilizes hCBS. In the presence of SAM, the C_m value (i.e., the concentration of urea required to unfold the CBS) increased from 2.9 ± 0.1 M to 4.6 ± 0.02 M.

Figure 1.6. Location of residue I278 in the context of the structure of the truncated, dimeric form of hCBS. View is cartoon representation (PyMOL, Delano Scientific Inc., CA) of hCBS with I278 (grey), the PLP cofactor (yellow) and heme cofactor (red) shown in stick representation.

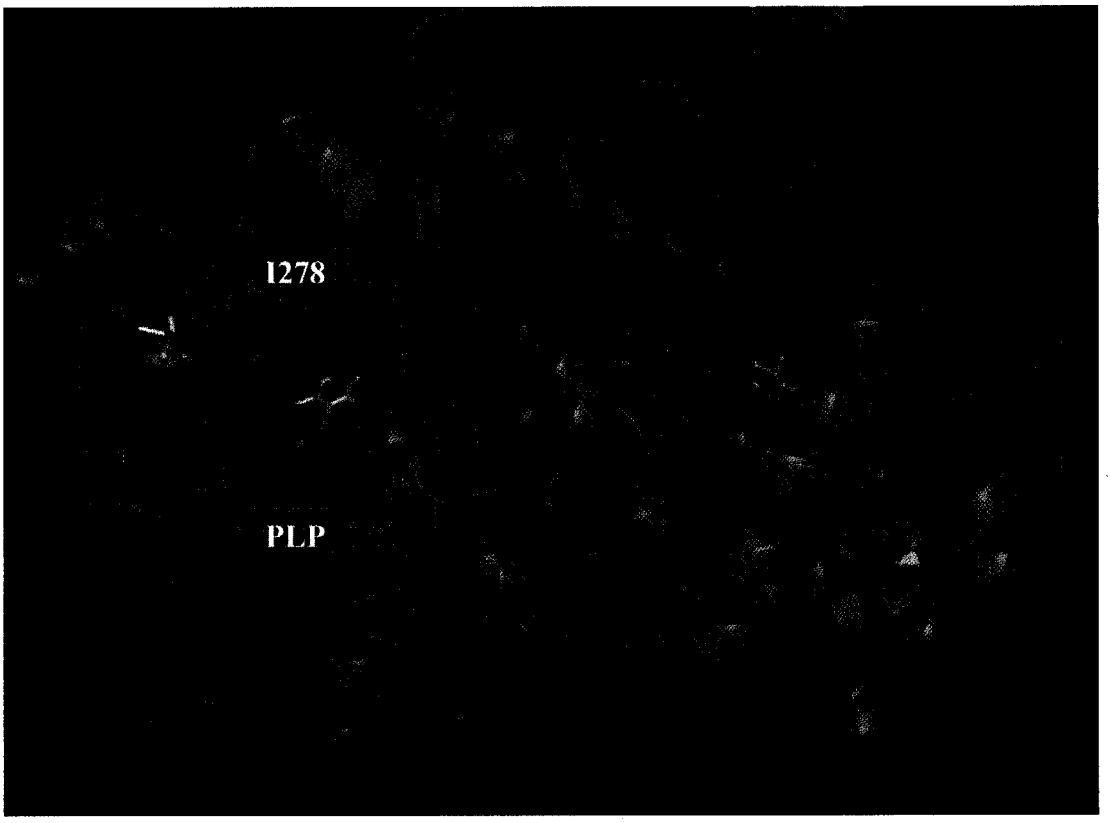
1278
PLP

Subsequently, a structural analogue for SAM, *S*-Adenosyl- L- Ethionine (SAE), was used to induce hCBS in Met^{-} Hcy^{+} grown cells (cells which are grown in a medium in which methionine is replaced by homocysteine) to distinguish between a chemical (through a methyl transfer) and structural role for SAM in the modulation of hCBS activity (Purdova *et al.,* 2006).

It was found that SAE activates and stablizes hCBS, suggesting that the stabilizing effect of SAM on cells is associated with binding (structural role) rather than methyl transfer to hCBS or some other target (chemical role) (Purdova *et al.,* 2006). SAM binds stoichiometrically to each subunit with a K_d of 7.4 ± 0.2 μM (Taoka *et al.,* 1999). Although the SAM-binding site has not been characterized, it has been localized to the regulatory domain as the truncated form of hCBS (residues 1-413) is not allosterically activated by SAM (Banerjee and Kabil, 1999; Shan *et al.,* 2001; Oliveriusová *et al.*, 2002; Meier *et al.,* 2003).

1.5.2. Redox Regulation

Although the role of the heme cofactor in hCBS is still an open question, a regulatory role has been proposed (Nozaki *et al.,* 2001). NMR spectroscopy revealed that changes in the oxidation state of the heme iron are sensed by the phosphorous nucleus of the PLP, as evidenced by ^{31}P chemical shift changes, demonstrating that the oxidation status of the heme is transmitted to PLP, approximately 20 Å distant (Nozaki *et al.,* 2001). Additionally, reduction of the ferric heme iron of hCBS by titanium citrate results in a approximately 2-fold decrease in enzyme activity (Banerjee *et al.*, 1998), although the physiological

relevance of this observation has not been demonstrated. The responsiveness of hCBS activity to changes in the oxidation state of the heme has led to the hypotheses that the heme cofactor of hCBS may be a redox sensor (Banerjee *et al.,* 2000). However, in a recent study by Burstyn *et al.,* 2004, it was shown that the redox behavior of the heme cofactor is regulated by pH, although in a physiologically non-relevant manner.

The crystal structure of the truncated, dimeric form of hCBS (htCBS) revealed the existence of a surface-exposed CXXC oxido-reductase motif comprising the two cysteine residues, Cys272 and Cys275, which may be involved in redox sensing (Meier *et al.,* 2001). The role(s) of this motif and the heme cofactor in modulating the redox responsiveness of the enzyme has been examined by mutagenesis of the cysteine residues in the CXXC motif and by generation of heme domain mutants, CBSΔN69 (Banerjee *et al.,* 2003). The C272A and C275S mutants have spectroscopic properties similar to those of the wild type enzyme and show similar redox sensitivity, thus excluding a role for these cysteine residues in the redox responsiveness of hCBS. In contrast, the heme-domain-deletion mutant, which retained most of the enzymatic activity of the wild type enzyme, was found to be insensitive to the presence of reducing agents, demonstrating the involvement of the heme cofactor in the proposed redox sensitivity of hCBS (Banerjee *et al.,* 2003). The intuitive metabolic rationale for activation of hCBS under conditions of oxidative stress, *i.e.* the physiological relevance of the proposed redox sensitivity of hCBS (Banerjee *et al.,* 2000), is that it would enhance conversion of methionine to cysteine; the limiting reagent in the synthesis of glutathione under oxidizing conditions.

1.6. Link between Cellular Methylation and Antioxidant Metabolism

In mammals, cellular methylation and antioxidant metabolism are linked by homocysteine, the common precursor of the transmethylation and transulfuration pathways (Purdova *et al.*, 2006). The coordinated regulation of methylation and antioxidant metabolism is achieved *via* the allosteric activation of hCBS by SAM (see earlier sections). Purdova *et al.* (2006) showed that under conditions of methionine restriction, glutathione levels are reduced, a phenomenon that is usually observed under pathological conditions that increase the oxidative stress of tissues, such as hepatocellular carcinoma and chronic steatohepatitis (Kruger *et al.*, 2004).

1.7. Abundance of Glutathione in Cells and Plasma

The ratio of the reduced (GSH) to oxidized (GSSG) forms of glutathione ([GSH]/[GSSG]), which is often used as an indicator of the cellular redox state, is approximately ten under normal physiological conditions (Tietze, 1969). This ratio is the major factor that determines the antioxidant capacity of cells, as glutathione is the predominant low-molecular weight thiol (can approach a concentration of 10 mM in some cell types) in animal cells. Most of the cellular glutathione (85-90%) is present in the cytosol, with the remainder in various organelles, including the mitochondria, nuclear matrix and peroxisomes (Lu, 2000). With the exception of bile acid, which may contain up to 10 mM GSH, the extracellular concentration of GSH is relatively low (*e.g.* 2-20 μM in plasma) (Jones, 2002). Cellular GSH levels are reduced markedly in response to protein malnutrition, oxidative stress, and many pathological conditions (Nörgren and Njälsson, 2005).

Glutathione is synthesized in two consecutive steps by the enzymes γ-glutamylcysteine synthetase (γ-GCS) and GSH synthetase in reactions (1) and (2), respectively, of Scheme 1.1. These reactions occur in virtually all cell types in animals, with the liver being the major producer and exporter of GSH (Wu *et al.*, 2004). The peptide bond formed by γ-GCS between the L-Glu and L-Cys residues is atypical in that it involves the γ-carboxyl group of the glutamate. This makes glutathione resistant to hydrolysis by most peptidases (Anderson, 1998), and partially explains its large intracellular concentration.

L-Glu + L-Cys + ATP ⟶ L-γ-Glu-Cys + ADP + Pi (1)

L-γ-Glu-Cys + Gly + ATP ⟶ L-γ-Glu-Cys-Gly (glutathione) + ADP + Pi (2)

Scheme 1.1. Glutathione biosynthesis catalyzed by γ-glutamylcysteine synthase (γ-GCS; 1) and glutathione synthase (GS; 2).

1.8. Regulation of GSH Biosynthesis

The biosynthesis of GSH can be regulated in two ways: either by the rate-determining enzyme γ-GCS or by the availability of its substrate amino acids. There are several factors that regulate the abundance and activity of γ-GCS in the cell. For example, it has been reported that oxidative or nitrosative stress, inflammatory cytokines, cancer, chemotherapy, ionizing radiation, heat shock, heavy metals, antioxidants and inhibition of γ-GCS itself increase either the γ-GCS transcription or change its activity in a variety of cells (Townsend *et al.,* 2003). In contrast, factors including hyperglycemia (elevated level

of blood glucose), erythropoietin, and γ-GCS phosphorylation decrease γ-GCS expression or activity.

The intracellular pool of L-Cys is relatively small (0.15–0.25 mmol/L), compared with the much larger concentration of GSH in cells, as noted above (Wu *et al.,* 2004). Thus, factors (*e.g.* insulin and growth factors) that stimulate L-Cys (and/or cystine) uptake by cells generally increase the intracellular GSH concentration (Lu, 2000). In addition, increasing the supply of L-Cys or its precursors (e.g., cystine, *N*-acetyl-L-cysteine or L-2-oxothiazolidine-4-carboxylate) *via* oral or intravenous administration, enhances GSH synthesis and prevents GSH deficiency in humans and animals under various nutritional and pathological conditions, including protein malnutrition, adult respiratory distress syndrome and HIV/AIDS (Nörgren and Njälsson, 2005). Since methionine catabolism, *via* the transsulfuration pathway, primarily in liver cells, provides L-Cys as a substrate for γ-GCS, dietary methionine can replace cysteine to support GSH synthesis *in vivo* (Purdova *et al.,* 2006).

1.9. The Physiological Roles of Glutathione

Glutathione participates in many cellular reactions. For example, GSH, as the predominant low molecular weight thiol, effectively scavenges free radicals and other reactive oxygen species (e.g., hydroxyl radical, lipid peroxyl radical, peroxynitrite, and hydrogen peroxide) directly and indirectly, through enzymatic reactions (Fang *et al.,* 2002). In such reactions, GSH is oxidized to form GSSG, which is then reduced to regenerate GSH by NADPH-dependent glutathione reductase. Oxidative stress, a deleterious imbalance between the production and removal of reactive oxygen/nitrogen

species, has been reported as an important risk factor in aging and associated disorders (Kruger *et al.,* 2004). Oxidative stress also plays a key role in the pathogenesis of many diseases, including cancer, inflammation, kwashiorkor (predominantly due to protein deficiency), seizure, Alzheimer's disease, Parkinson's disease, sickle cell anemia, liver disease, cystic fibrosis, HIV/AIDS, infection, heart attack, stroke and diabetes (Purdova *et al.*, 2006). Another role of GSH is its reaction with various electrophiles, physiological metabolites (e.g. estrogen, melanin, prostaglandins, and leukotrienes), and xenobiotics (e.g. bromobenzene and acetaminophen), ultimately converting them into mercapturates, glutathione conjugates, to be excreted from body thereby avoiding their deleterious effects (Fang *et al.,* 2002). These reactions are carried out by the glutathione-*S*-transferases, a family of enzymes involved in the conjugation of GSH to various electrophiles. Another role of GSH is to serve as a substrate for formaldehyde dehydrogenase, which converts formaldehyde, a carcinogen, and GSH to *S*-formyl-glutathione (Townsend *et al.*, 2003). It is also important to note that a reduction in the GSH/GSSG ratio activates several signalling pathways including those that enhance apoptosis, thereby reducing cell proliferation and increasing cell death (Purdova *et al.,* 2006). Moreover, Haddad *et al.,* (2000) reported that the hypoxic activation of the oxygen- and redox-sensitive transcription factors, including hypoxic inducible factor-1α (HIF-1α) and nuclear factor-κB (NF-κB) is redox-sensitive (referring to the hypoxic activation) and therefore strongly regulated by the GSH/GSSG equilibrium. Glutathione is also involved in the transport of amino acids, *via* the γ-glutamyl cycle, and maintenance of the cellular pool of reduced ascorbic acid (Anderson 1998).

1.10. Hypothesis

Studies on hCBS have largely focused on the identification of homocystinuria-associated mutations and unravelling the structural details of the enzyme with respect to the location and roles of residues corresponding to these mutations (Mudd *et al.,* 1985; Kraus, 1994; Banerjee and Kabil, 1999; Kraus *et al.*, 1999; Kruger *et al.*, 2001; Meier *et al.*, 2001; Meier *et al.*, 2003; Kraus and Miles, 2004). However, there is little information, in either *in vitro* or *in vivo* systems, on the functional link between the transulfuration and glutathione biosynthetic pathways, with regards to the effect of these homocystinuria-associated mutations.

The central hypothesis of this thesis is that that those naturally-occurring missense mutations (G148R, G259S, G305R, G307S and I278T), in proximity to the active site of the enzyme, lead to a dysfunctional enzyme and, ultimately, to reduced levels of cellular glutathione, compared to the wild-type enzyme, upon transient transfection and over-expression in mammalian cells.

1.11. Specific Objectives

The goal of my thesis was to investigate the effect of a series of naturally-occurring missense mutations in the catalytic domain of hCBS on the activity of this enzyme and on the cellular glutathione status.

To achieve this objective, two methods were developed:

1. a novel and sensitive assay for quantification of picomole levels of glutathione in cell lysates was modified and assessed (Chapter 1) and

2. a convenient and less-expensive bacterial expression system that would produce enough of the recombinant enzyme for subsequent steady state kinetic analyses of wild type and mutant hCBS in an *in vitro* system (Chapter 2).

The outcomes of this research will give insight to better understand the metabolic link between the transulfuration and the glutathione biosynthetic pathways. Identifying pertinent mutations of hCBS with clear effects on cellular glutathione status could lead to the discovery of therapeutic strategies for the maintenance of antioxidant status and the prevention of cardiovascular diseases associated with elevated plasma homocysteine levels.

Chapter Two

Coupled Enzyme NADPH-recycling Assay for Measuring Total and Oxidized Glutathione: A Comparison with Other Methods

2.1. INTRODUCTION

Glutathione (L-γ-glutamyl-L-cysteinyl-glycine) is the most abundant low molecular weight, non-protein thiol present in plant and animal cells (Meister and Anderson 1984). It is present in the cell in both reduced (GSH) or oxidized (GSSG) forms and can attain intracellular concentrations in the millimolar range (Kaplowitz *et al.,* 1985). The proportion of GSH to GSSG varies with tissue types and the oxidative status of the cell (Sies *et al.,* 1979; Fujikawa *et al.,* 1994). In general, under normal metabolic conditions, cells maintain more than 90% of their total glutathione as GSH. The ratio of GSH/GSSG is maintained by the action of the ubiquitous NADPH-dependent enzyme, glutathione reductase (GR; E.C.1.8.1.7) (Williams 1976). The tripeptide is involved in detoxifying reactions, scavenging intracellular peroxides and conjugation to electrophilic metabolites of xenobiotics by the action of glutathione S-transferases (Kaplowitz *et al.,* 1985). The ratio of GSH/GSSG is commonly used as a measure of cellular oxidative stress.

Several techniques for measuring glutathione, employing a variety of detection methods, have been described, including a) spectrophotometric (Tietze 1969; Griffith 1980; Ellman 1959), bioluminescence (Mourad *et al.,* 2000) or fluorescence (Lewicki *et al* 2006) based enzymatic assays, b) liquid chromatography followed by electrochemical detection (Harvey *et al.,* 1980; Bousquet *et al.,* 1989; Lakritz *et al.,* 1997) or mass spectroscopy (Rellán-Álvarez *et al.,* 2006; Seiwert and Karst 2007) and c) capillary electrophoresis (Serru *et al.,* 2001) and NMR (Reglinski *et al.,* 1999). Chromatographic methods have the advantage of simultaneous separation and quantitation of both GSH and GSSG. However, these methods usually require extensive prior derivatization with either iodoacetic acid (Reed *et al.,* 1980) or N-ethylmaleimide (Giustarini *et al.,* 2003) and

subsequent treatment with 2,4-dinitrofluorobenzene. In contrast, spectroscopic methods are more amenable to high throughput analysis and are more generally accessible.

The conventional glutathione assay, developed by Tietze (1969) and modified by Griffith (1980), utilizes GR to reduce GSSG and make it available for an uncatalyzed reaction with DTNB (Scheme 2.1). Recently (Neumann *et al.,* 2003), an enzymatic method has been developed which recycles the nicotinamide adenine dinucleotide phosphate (NADPH) in the original method. This method couples glucose-6-phosphate dehydrogenase (G6PDH) with GR, thereby allowing the continuous regeneration of the limiting reagent NADPH from $NADP^+$ (Scheme 2.2). The assay can detect picomole levels of GSH and GSSG.

At millimolar intracellular concentrations, GSH is easily measured in whole cell lysates. However, indication of oxidative stress requires measurement of the much less prevalent GSSG. Therefore methods that measure glutathione in cells strive for more accurate measures of GSSG. The present study refines the method of Neumann et al. (2003) by optimizing the conditions in order to minimize G6PDH and G6P usage, thereby reducing its cost to make it more amenable as a high throughput technique. The accuracy and detection limit of this assay is compared with the standard GR-based assay (Scheme 2.1) as well as HPLC coupled with electrochemical detection; the method currently considered to be the most sensitive (Kruusma *et al.,* 2006).

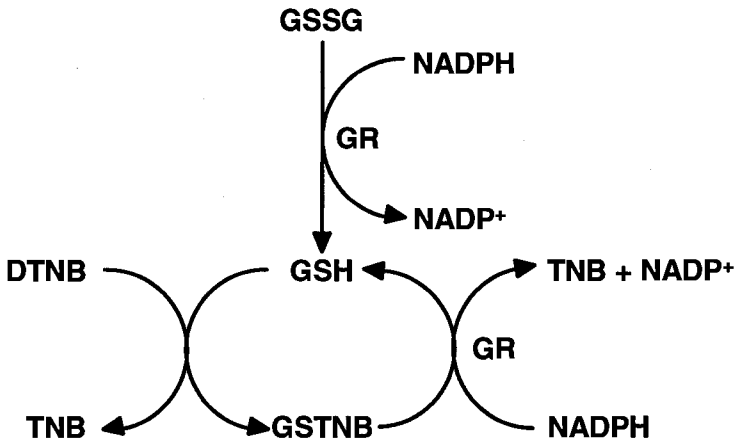

Scheme 2.1. Conventional enzymatic method for the quantification of GSH and GSSG based on the method of Tietz (1969). GSTNB = the disulfide product of the reaction of GSH with 5, 5'-dithio-bis (2-nitrobenzoic acid) (DTNB; Ellman's reagent (Ellman 1959)). 5'-thionitrobenzoic acid (TNB) is the product measured at 412 nm. NADPH = reduced nicotinamide adenine dinucleotide phosphate, $NADP^+$ = oxidized nicotinamide adenine dinucleotide phosphate.

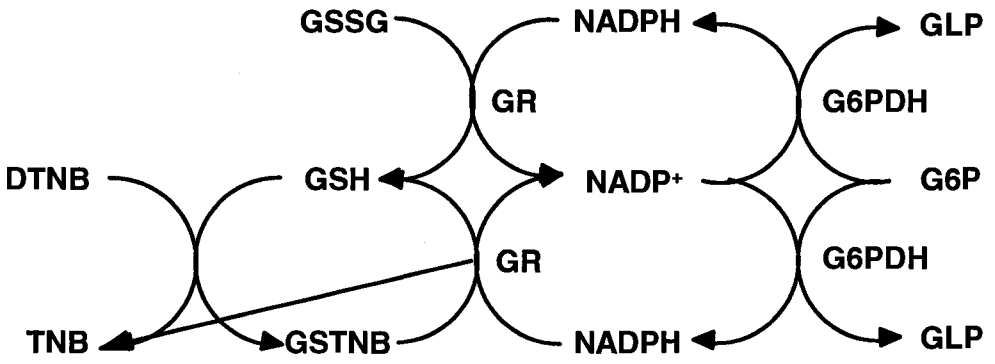

Scheme 2.2. The NADPH recycling assay, incorporating glucose-6-phosphate dehydrogenase (G6PDH) and glucose-6-phosphate (G6P), for the quantification of GSH and GSSG based on the method of Neumann *et al.* (2003). GLP = D-glucono-1, 5-lactone-6-phosphate, NADPH = reduced nicotinamide adenine dinucleotide phosphate, $NADP^+$ = oxidized nicotinamide adenine dinucleotide phosphate.

2.2. MATERIALS AND METHODS

2.2.1. Chemicals and Cell Culture

All chemicals and kits were purchased from Sigma (St. Louis, Missouri) unless specified below. Baker's yeast G6PDH (Type VII) was purchased from Sigma and used in the recycling assay. Human chronic myelogenous leukemia (K562), human embryonic kidney (HEK293) and mouse embryonic fibroblast (3T3) cells were purchased from the American Type Culture Collection (Manassas, Virginia). An adherent clone of rat adrenal pheochromocytoma (PC-12AC) was obtained from Dr. Steffany Bennett (Biochemistry, Microbiology and Immunology, University of Ottawa, Ottawa). Cell culture medium, serum and antibiotics/antimycotics were purchased from Invitrogen (Carlsbad, California). Cultures were maintained at a density of 1 X 10^6 cells/mL at 37°C and 5% CO_2 in a humidified tissue culture incubator (Thermo Forma, Marietta, Ohio). Treatment of cells with various concentrations of the glutathione synthesis inhibitor buthionine sulfoxamine (BSO; 0, 0.02, 0.1 and 0.2 mM) was performed in 6-well plates for 24 hours.

2.2.2. Cell Lysis and Protein Determination

Cells were were harvested by cell lifting and centrifuged at 5,000 g for 5 minutes. Cells were lysed 1:5 (w/v) in ice-cold 5% sulfosalicylic acid (SSA; previously bubbled with nitrogen gas for 10 minutes), then bubbled with nitrogen gas for 10 seconds and centrifuged at 16,000 g in an Eppendorf microcentrifuge for 5 minutes. The supernatant was collected for GSH and GSSG analysis. Cell pellets were saved for protein determination and stored at -80°C. Cell pellets were resuspended in the same volume of

0.5 M potassium phosphate buffer (pH 7.0) as acid that cells were lysed in. Total protein was determined using the Bio-Rad Protein Assay reagent according to the manufacturer's protocol.

2.2.3. Enzymatic Assays for Glutathione

The conventional assay for glutathione, based on the reaction of glutathione with DTNB (Tietze 1969) was adapted for the microplate reader (100 µL total volume; Spectramax 340^{384PC} (Molecular Devices, Sunnyvale, CA)). Aliquots of cell lysate supernatant were diluted 1:20 (v/v) with water and used immediately for the measurement of total glutathione equivalents (GSH + 2 GSSG; two moles of GSH can be produced from each mole of GSSG). GSH equivalents were determined by following the rate of reduction of DTNB to TNB by GSH at 412 nm and comparing this with GSH and GSSG standard curves. Samples were added to an assay medium containing 100 mM sodium phosphate buffer (pH 7.5), 5 mM sodium EDTA, 0.21 mM NADPH, and 0.6 mM DTNB, and then the reaction was started with the addition of 0.5 U/mL GR. The reaction was allowed to proceed for 10 min and the data were fit by linear regression to determine the rate of TNB formation. In both the conventional and NADPH-recycling methods, GSSG can be measured by first derivatizing GSH with either 2-vinylpyridine (Griffith 1980) or 1-methyl-4-vinyl-pyridinium (Shaik and Mehvar 2006), removing GSH from reaction with DTNB. In this study, GSSG alone was measured separately following derivatization of GSH with 2-vinylpyridine. Samples of cell lysate (undiluted; 500 µL) were mixed with 100 µL of 0.5 M 2-vinylpyridine and 1 mL of 0.5 M KPi, pH 7.0. After derivatization for 1 hour at room temperature, GSSG was measured (as 2 GSH) using the assay above. The

recycling assay was the same as the conventional assay with the inclusion of 20 mM glucose-6-phosphate (G6P) and 0.2U/mL glucose-6-phosphate dehydrogenase (G6PDH). Standards of GSH and GSSG were created from a 1:50 dilution of 1 mM stock solutions to achieve the lowest concentration that can be detected with the assay. Standard curves of 0 to 1.6 nmoles of GSH or 0 to 0.8 nmoles of GSSG for the microplate assays and 0 to 0.8 nmoles of GSH or 0 to 0.4 nmoles of GSSG for HPLC with electrochemical detection (EC-HPLC) were created.

2.2.4. HPLC Assay for Glutathione

Chromatographic conditions were modified from those described by Lakritz *et al.*, 1997. Samples were chromatographed by loading and injecting 100 µL of sample into HPLC after 5 minutes of stabilization with a mobile phase containing 50 mM sodium phosphate (monobasic), 0.05 mM octane sulfonic acid, 2 mM potassium chloride and 2% acetonitrile, adjusted to a pH of 2.5, and a flow rate of 1 mL/min. The electrode was set at +0.88 V potential and the full-scale output was set at 0.1 µA. The chromatogram peaks for GSH and GSSG were analyzed using Star Workstation chromatography software (Varian Inc., Palo Alto, California). The GSH and GSSG content in samples were determined by comparing integrated peak areas to standard curves of GSH and GSSG respectively.

2.2.5. Data Analysis and Statistics

An assessment of the sensitivity of the NADPH-recycling assay was made in comparison to other methods of glutathione measurement. The limits of detection (LoD) and quantification (LoQ) were calculated from the slope (*a*) and intercept values (*b*) of the

linearity curve, and the standard deviation of the intercept (S.D.*b*). Limits were expressed, respectively, as LoD = $(b + 3\ \text{S.D.}b)/a$ and LoQ = $(b + 10\ \text{S.D.}b)/a$ according to MacDougall (1980).

Statistical comparisons of multiple means were performed using ANOVA with a post hoc analysis of means based on Tukey's test. For comparisons involving only two means, a two-tailed, unpaired t-test was used. Data are presented as means ± standard error of the mean of ≥ three replications.

2.3. RESULTS

The optimal concentrations of G6P and G6PDH required for the NADPH-recycling assay were determined to be 20 mM and 0.2 U/mL respectively (Figures 2.1A and B). Beyond these concentrations, further addition of substrate or enzyme had no effect on the rate of TNB^- production. These concentrations were used for all subsequent experiments using the recycling assay.

GSH and GSSG standard curves obtained, using as standards for conventional, recycling and EC-HPLC assays for glutathione are presented in Figures 2.2A, 2.2B and 2.3 respectively. The slope of the GSH curve was 1.6-fold higher in the recycling assay than in the conventional one (Figure 2.2A). This resulted in greater sensitivity of the recycling assay than the conventional assay at higher concentrations of GSH. For GSSG, the slope of the NADPH-recycling assay was only slightly higher than the conventional one, suggesting an equal sensitivity for GSSG. All three assays for glutathione were capable of detecting as little as 2 μM glutathione. The limits of detection (LoD) for the recycling assay were 2.9- and 2.7-fold greater than the conventional assay for GSH and GSSG respectively (Table 2.1). Likewise, the limits of quantification (LoQ) for the recycling assay were approximately 5-fold lower than for the conventional assay for both GSH and GSSG. LoD and LoQ results must be interpreted with caution as they tend to magnify small differences in sensitivity. Differences suggested by LoD and LoQ between recycling and conventional assays may not be significant at lower glutathione concentrations. The recycling assay was also more reproducible than the conventional assay for GSH and GSSG (Table 2.1) and more reproducible for GSH than EC-HPLC. It is interesting to note that the error was larger for the conventional assay at higher GSH concentrations. The NADPH-recycling

Figure 2.1. Determination of the optimal concentrations of **A**) G6P and **B**) G6PDH for the NADPH-recycling method. Assay conditions: 0.21 mM NADPH, 0.6 mM DTNB, 0.5 U/mL GR, 100 mM sodium phosphate buffer (pH 7.5), 5 mM sodium EDTA and varying concentrations of either G6P (**A**; 0 to 22.5 mM with 0.2 U/mL G6PDH) or G6PDH (**B**; 0 to 0.6 U/mL with 22.5 mM G6P). The results for this optimization are obtained from a single replication.

A

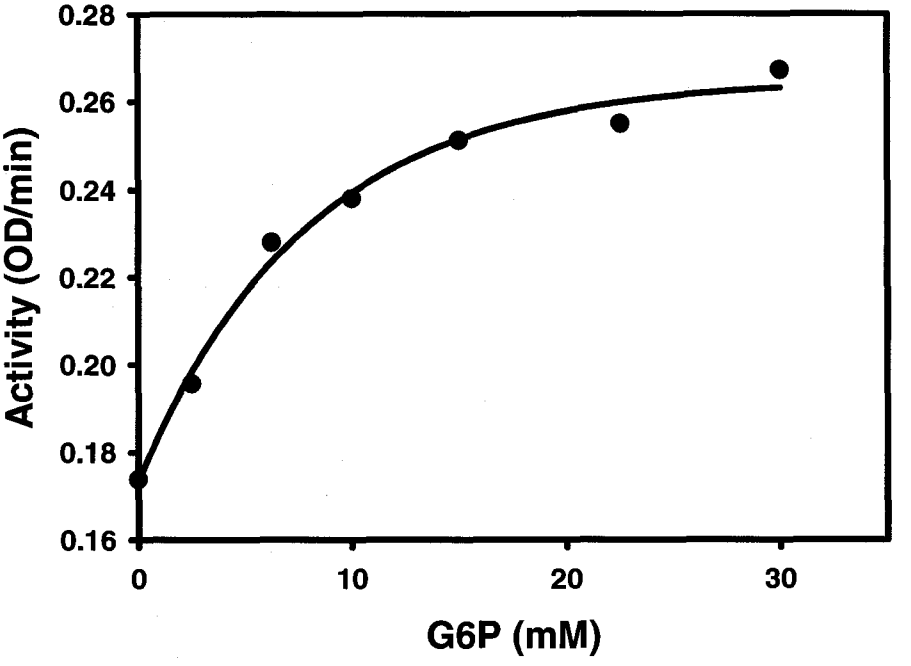
0.28
0.26
0.24
0.22
0.20
0.18
0.16
Activity (OD/min)
0
10
20
30
G6P (mM)

B

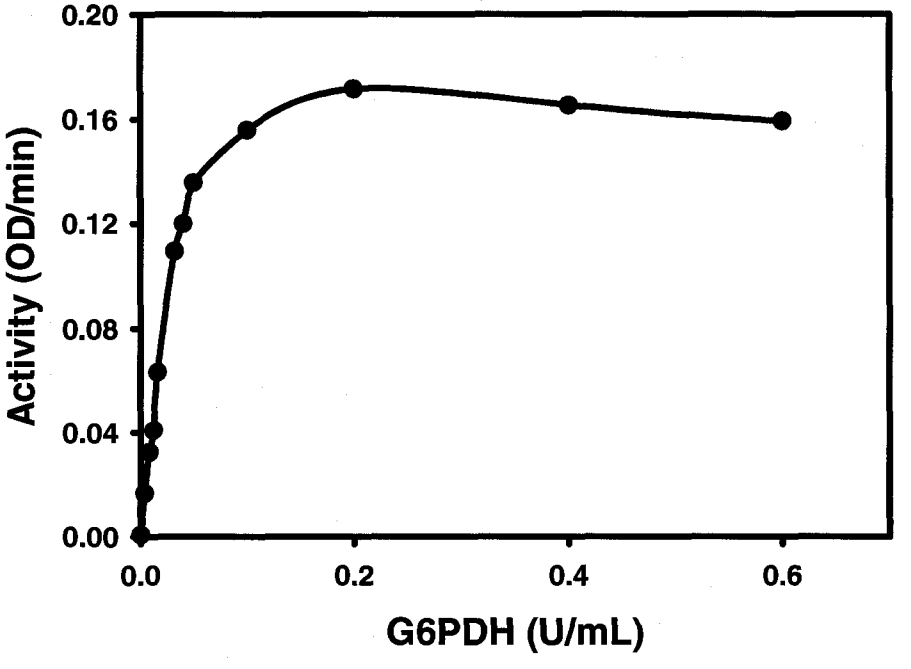
0.20
0.16
0.12
0.08
0.04
0.00
Activity (OD/min)
0.0
0.2
0.4
0.6
G6PDH (U/mL)

Figure 2.2. Standard curves for **A**) GSH (0 to 1.6 nmoles) or **B**) GSSG (0 to 0.8 nmoles), based on the conventional, GR-based glutathione assay (open circle) and the NADPH-recycling method (closed circle). Assay conditions: 0.21 mM NADPH, 0.6 mM DTNB, 0.2 U/mL G6PDH, 0.5 U/mL GR, 100 mM sodium phosphate buffer (pH 7.5), 5 mM sodium EDTA; and 20 mM G6P and 0.2 U/mL G6PDH for the recycling assay. Means ± standard error of the mean ($n \geq 3$) are shown. Many error bars are hidden under symbols.

A

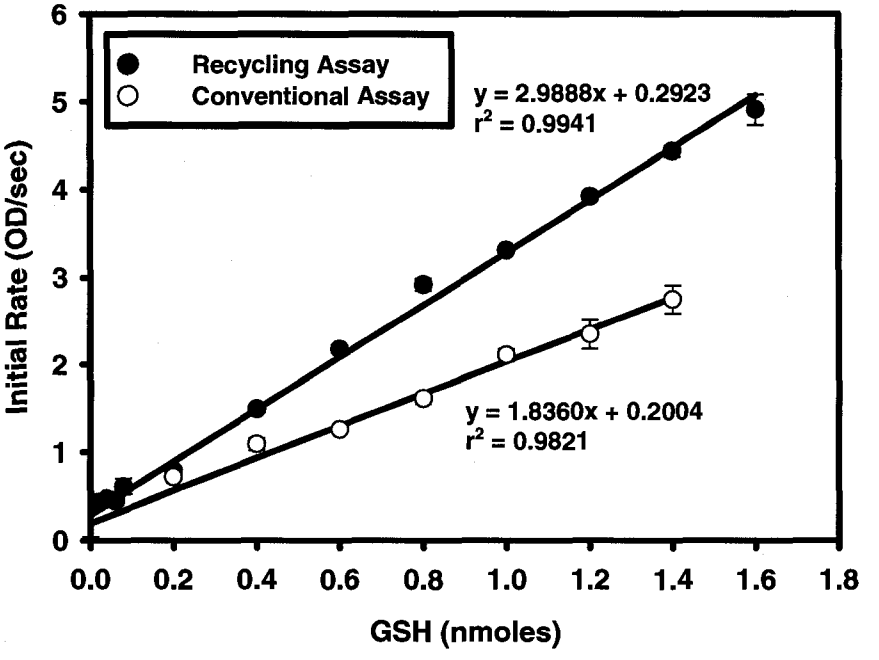
Recycling Assay
Conventional Assay
y = 2.9888x + 0.2923
r² = 0.9941
y = 1.8360x + 0.2004
r² = 0.9821
Initial Rate (OD/sec)
GSH (nmoles)
0
1
2
3
4
5
6
0.0
0.2
0.4
0.6
0.8
1.0
1.2
1.4
1.6
1.8

B

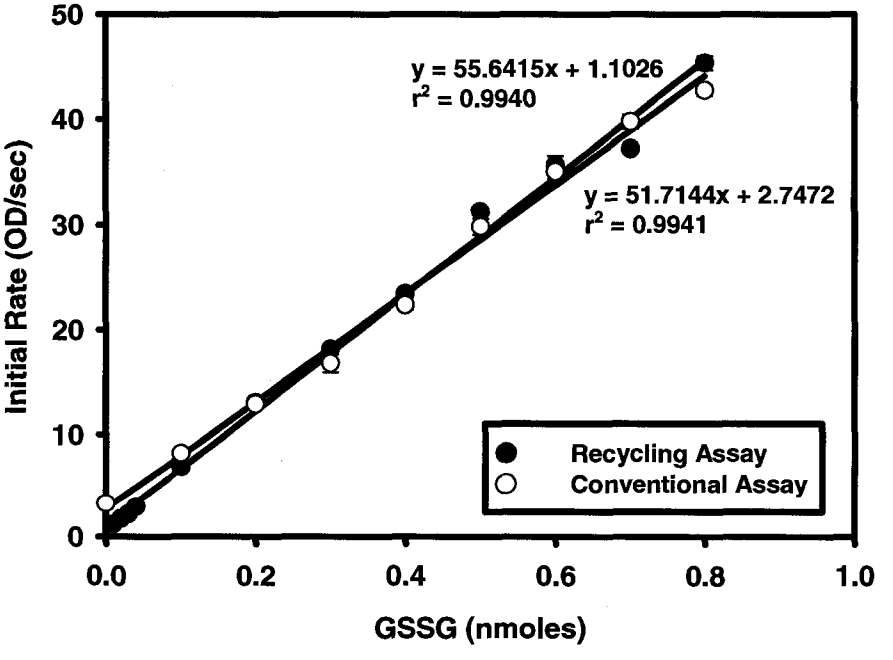
y = 55.6415x + 1.1026
r² = 0.9940
y = 51.7144x + 2.7472
r² = 0.9941
Recycling Assay
Conventional Assay
Initial Rate (OD/sec)
GSSG (nmoles)
0
10
20
30
40
50
0.0
0.2
0.4
0.6
0.8
1.0

Figure 2.3. Standard curves of GSH (0 to 0.8 nmoles) and GSSG (0 to 0.4 nmoles) based on the HPLC electrochemical detection parameters outlined in Materials and Methods. Means ± standard error of the mean ($n \geq 3$) are shown. Many error bars are hidden under symbols.

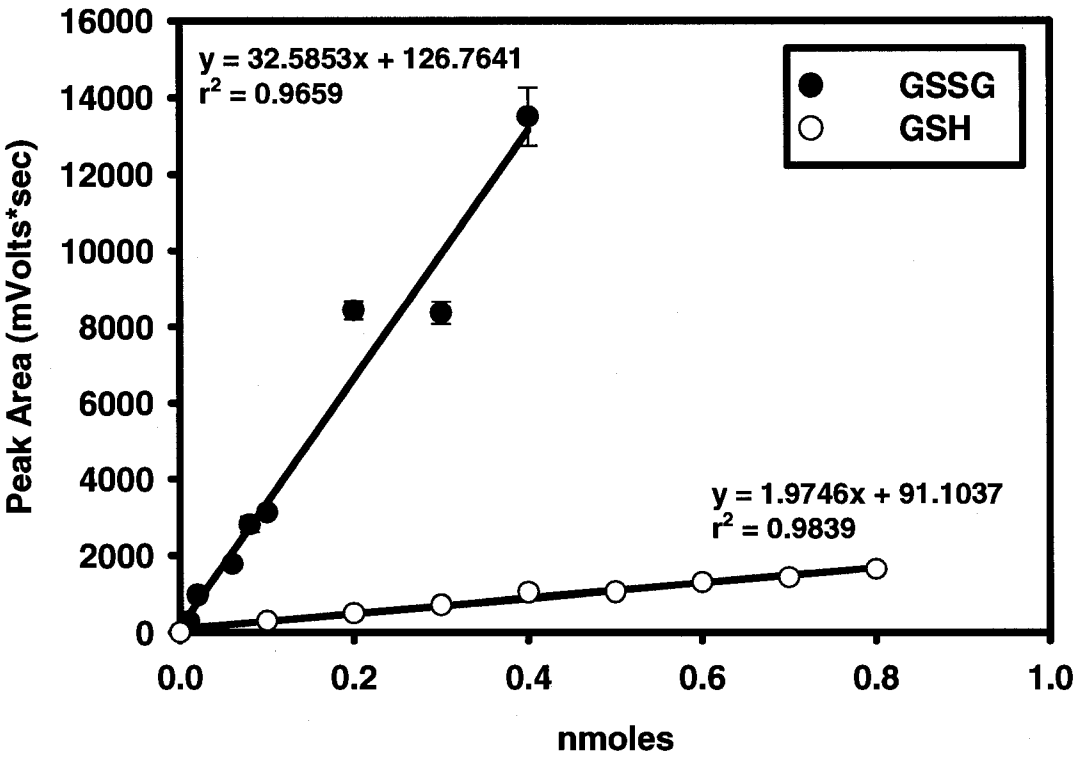
y = 32.5853x + 126.7641
r2 = 0.9659
GSSG
GSH
y = 1.9746x + 91.1037
r2 = 0.9839
Peak Area (mVolts*sec)
16000
14000
12000
10000
8000
6000
4000
2000
0
0.0
0.2
0.4
0.6
0.8
1.0
nmoles

Table 2.1. Main validation parameters of the three methods of measuring GSH and GSSG

Validation parameter	Conventional		Recycling		EC-HPLC	
	GSH	GSSG	GSH	GSSG	GSH	GSSG
Linearity range	0.2-1.4 nmoles $0.98 < R^2 < 1.00$	0.01-0.80 nmoles $0.99 < R^2 < 1.00$	0.02-1.60 nmoles $0.99 < R^2 < 1.00$	0.01-0.80 nmoles $0.99 < R^2 < 1.00$	0.10-0.80 nmoles $0.98 < R^2 < 1.00$	0.01-0.40 nmoles $0.96 < R^2 < 1.00$
Slope	1.8	51.7	3.0	55.6	2	32.6
Intercept	0.20	2.8	0.30	1.1	91.1	126.8
Limit of detection[a]	0.40	0.08	0.13	0.03	0.12	0.10
Limit of quantification[a]	1.0	0.14	0.21	0.05	0.30	0.24
Reproducibility	2.7 to 6.0%	2.8 to 110.1%	0.6 to 1.7%	0.6 to 9.1%	3.0 to 11.1%	3.3 to 4.1%

[a]The limits of detection (LoD) and quantification (LoQ) were calculated as outlined in Materials and Methods.

[b]Reproducibility was calculated from the means and standard deviation of glutathione measures (nmoles/μg protein) in cell lysates from all cell lines and expressed as a range of percentages (S.D./mean X 100).

assay may therefore be more sensitive at higher GSH than the conventional assay.

The levels of GSH and GSSG were measured in four diverse and commonly used cell lines by both the NADPH-recycling and conventional glutathione assays (Table 2.1). The NADPH-recycling assay measured consistently higher levels of both GSH and GSSG with smaller differences occurring in the levels of GSSG between NADPH-recycling and conventional assays. Differences in detection limits of GSH and GSSG in whole cell lysates between recycling and conventional assays were reflected in differences in the standard curves between the two methods. In general, the NADPH-recycling method detected two- to thirteen-fold more GSH in cell lysates than the conventional method. Likewise, the recycling method detected 79- to 1,252-fold more GSH in cell lysates than EC-HPLC (Table 2.1). With the exception of PC12AC cells, the results for GSSG between the NADPH-recycling and EC-HPLC methods were comparable.

In order to determine whether changes in glutathione concentrations *in vivo* were measurable by the recycling method, HEK293 cells were treated with BSO, and glutathione was measured by both conventional and NADPH-recycling microplate assays. BSO is inhibitor of γ-glutamylcysteine synthase, the enzyme that catalyzes the first and rate-limiting step of glutathione biosynthesis pathway; the linkage of cysteine and glutamate. Levels of glutathione measurable by both assays are presented in table 2.3. The recycling method measured 1.2- to 13.5-fold more total glutathione in untreated cells than the conventional method, due to the higher upper limit of the NADPH-recycling assay. With depletion of glutathione with BSO, detectable levels of total glutathione were similar for both assays. Statistically significant depletion of glutathione with BSO was only detectable with the highest BSO concentration (0.2 mM) using the conventional method.

Table 2.2. Reduced (GSH), oxidized (GSSG) and total glutathione from lysates of four cell lines as measured by the a) conventional glutathione, b) the NADPH-recycling glutathione and c) the EC-HPLC assays. Total, reduced and oxidized glutathione concentrations are normalized by calculating actual amounts of glutathione per mass of protein. Values are means ± standard error of the mean (≥ 3 replications).

			Cell Line			
			K562	**PC12AC**	**HEK293**	**3T3**
Enzymatic Assays						
Total Protein (μg/μL)			0.70	0.74	0.60	0.60
Reduced glutathione (GSH)	**mM**	**Conventional**	3.4 ± 0.1	1.20 ± 0.04	2.70 ± 0.04	2.70 ± 0.05
		Recycling	7.30 ± 0.03	17.2 ± 0.1	3.20 ± 0.02	7.40 ± 0.07
	nmoles/μg protein	**Conventional**	4.7 ± 0.2	1.70 ± 0.05	4.70 ± 0.07	4.90 ± 0.08
		Recycling	10.00 ± 0.04	23.1 ± 0.1	5.70 ± 0.03	13.2 ± 0.1
Oxidized glutathione (GSSG)	**mM**	**Conventional**	$(5 \pm 3) \times 10^{-3}$	$(4.00 \pm 0.07) \times 10^{-2}$	$(6 \pm 1) \times 10^{-3}$	$(1.0 \pm 0.1) \times 10^{-2}$
		Recycling	$(6.0 \pm 0.3) \times 10^{-4}$	$(5.0 \pm 0.2) \times 10^{-2}$	$(7.0 \pm 0.1) \times 10^{-3}$	$(1.00 \pm 0.04) \times 10^{-2}$
	nmoles/μg protein	**Conventional**	$(7 \pm 4) \times 10^{-3}$	$(6.00 \pm 0.09) \times 10^{-2}$	$(1.0 \pm 0.2) \times 10^{-2}$	$(2.0 \pm 0.2) \times 10^{-2}$
		Recycling	$(8.0 \pm 0.4) \times 10^{-3}$	$(6.00 \pm 0.02) \times 10^{-2}$	$(1.20 \pm 0.02) \times 10^{-2}$	$(2.00 \pm 0.07) \times 10^{-2}$
Total Glutathione	**mM**	**Conventional**	3.4 ± 0.1	1.30 ± 0.04	2.70 ± 0.04	2.70 ± 0.04
		Recycling	7.30 ± 0.03	17.2 ± 0.1	3.20 ± 0.02	7.40 ± 0.07
	nmoles/μg protein	**Conventional**	4.7 ± 0.2	1.70 ± 0.05	4.80 ± 0.07	4.90 ± 0.09
		Recycling	10.00 ± 0.03	23.2 ± 0.1	5.80 ± 0.07	13.3 ± 0.1
EC-HPLC Assay						
Total Protein (μg/μL)			0.70	0.62	0.50	0.94
Reduced glutathione (GSH)	**mM**		$(4.00 \pm 0.02) \times 10^{-2}$	$(1 \pm 0.04) \times 10^{-2}$	$(4.00 \pm 0..06) \times 10^{-2}$	0.12 ± 0.003
	nmoles/μg protein		$(5.0 \pm 3.4) \times 10^{-2}$	$(2.00 \pm 0.06) \times 10^{-2}$	$(7.0 \pm 0.1) \times 10^{-2}$	0.12 ± 0.003
Oxidized glutathione (GSSG)	**mM**		$(8.0 \pm 0.2) \times 10^{-3}$	$(2.00 \pm 0.05) \times 10^{-3}$	$(7.0 \pm 0.1) \times 10^{-3}$	$(7.0 \pm 0.2) \times 10^{-3}$
	nmoles/μg protein		$(1.00 \pm 0.03) \times 10^{-4}$	$(4.00 \pm 0.08) \times 10^{-3}$	$(2.00 \pm 0.03) \times 10^{-2}$	$(7.0 \pm 0.2) \times 10^{-3}$

Table 2.3. Total glutathione measured from HEK293 cell lysates after treating with various concentration of BSO using the conventional and NADPH-recycling recycling glutathione assays. This experiment was done to verify that the glutathione actually measured was synthesized *in vivo* and did not come from other sources. Values are means ± standard error of the mean (≥ 3 replications). (a) differs from conventional control (0 mM BSO) at $p < 0.05$; (b) differs from conventional assay at $p < 0.01$; (c) differs from NADPH-recycling assay control (0 mM BSO) at $p < 0.05$; (b) differs from NADPH-recycling assay control (0 mM BSO) at $p < 0.01$.

Assay	BSO (mM)	Total glutathione (mM)	Total protein (μg/μL)	Total glutathione/total protein (μmol/μg)
Conventional	0	1.40 ± 0.07	10.2	0.140 ± 0.007
	0.02	1.20 ± 0.03	9.2	0.130 ± 0.004
	0.1	0.300 ± 0.004	9.7	0.030 ± 0.004
	0.2	0.20 ± 0.01	8.5	0.020 ± 0.002 **(a)**
Recycling	0	14.0 ± 0.2	10.2	1.40 ± 0.02 **(b)**
	0.02	1.10 ± 0.03	9.2	0.120 ± 0.003 **(c)**
	0.1	0.30 ± 0.02	9.7	0.030 ± 0.001 **(d)**
	0.2	0.20 ± 0.01	8.5	0.020 ± 0.002 **(d)**

2.4. DISCUSSION

Total glutathione can be determined from cell lysates and tissue samples using the conventional GR-based assay developed by Tietze (1969). However, the information about the accuracy of this method, especially at high (when rates are too short to measure accurately prior to plateau) or low (when rates are too low that they are indistinguishable from background) concentrations, is lacking. Therefore, a NADPH-regenerating system was coupled to GR by Neumann *et al.* (2003), with the goal of lowering the possibility for substrate inhibition of GR by high levels of NADPH in the initial phase of the reaction. However, this assay was not compared to other methods for its linear range and optimal conditions. Therefore, this is the first study to assess the NADPH-recycling assay in comparison with, not only the conventional GR-based assay, but with EC-HPLC, the method that is considered to be the most sensitive for glutathione measurement (Kruusma *et al.,* 2006).

The conditions of the NADPH-recycling method were investigated and it was found that the optimal concentrations of G6P and G6PDH required for this assay were 20 mM and 0.2 U/mL, respectively. While the final concentration of G6P required was found to be almost 20-fold higher than that utilized by Neumann *et al.* (2003), the amount of G6PDH was found to be 16-fold less. This means that very little of the (relatively) expensive coupling enzyme is required for the NADPH-recycling method and that with more G6P, the assay has a longer running time. The increased linear range of the recycling assay was a product of the longer reaction time, enabled by the constant availability of NADPH. Unlike the conventional assay, the reaction progress curve in the NADPH-recycling assay did not plateau until thirty to forty minutes after initiation (data not shown). It was also

confirmed that DTNB and G6P do not interact to contribute to the increase in absorbance (data not shown). This method does not require exogenous supplementation with $NADP^+$ to prevent depletion of NADPH in the assay as was required in the original assay by Neumann *et al.* (2003). With the use of minimal amounts of NADPH in the assay, an initial ten minute pre-incubation period at room temperature in order to ensure that $NADP^+$ is completely reduced to NADPH was also found not to be required. G6PDH had kinetics to rapidly recycle $NADP^+$ to an optimal NADPH concentration for GR. Therefore, recycling allows a low, non-inhibitory concentration of NADPH to be used in the assay (Elliott *et al.,* 1992).

The results suggest that NADPH-recycling assay may be a more accurate method for the measurement of total and reduced glutathione but may have a similar accuracy for oxidized glutathione. The differences in the slopes of the GSH standard curves, in comparison to the equal slopes of the GSSG standard curves, suggest that GR has very high efficiency in recycling both GSSG and GS-TNB. With continual recycling of NADPH, the rate at which GR produces GSH (for reaction with DTNB) from GS-TNB greatly augments that which can be produced from GSH alone. This may mean that the conventional assay may have sufficient amounts of NADPH for recycling GSSG, but insufficient amounts to recycle GS-TNB (Scheme 2.1). With higher concentrations of GSSG, a separation in standard curves between conventional and NADPH-recycling assays may be seen.

In summary, it is observed that the NADPH-recycling assay has greater sensitivity than the conventional assay and EC-HPLC. Fourteen-fold and four-fold more total glutathione was detected using the NADPH-recycling assay than the conventional method

and EC-HPLC respectively. The assay also guarantees that NADPH is regenerated from $NADP^+$ at a rate that will not cause product inhibition of GR. This makes the recycling assay more amenable for high throughput assays at a minimal cost.

Chapter Three

Development of an Improved System for the Expression and Purification of Recombinant Human Cystathionine β-Synthase in *E. coli*

3.1. INTRODUCTION

Human CBS (hCBS) (EC. 4.2.1.22) is a homotetrameric protein with a subunit molecular weight of 63 KDa. Each of the subunits comprises 551 amino acids and a catalytic pyridoxal 5'-phosphate (PLP) cofactor (Mudd *et al.,* 1995; Clark *et al.,* 1998). Mammalian CBS is unique as it is the only PLP-dependent enzyme to also contain a heme cofactor. A regulatory role has been proposed for the heme (Banerjee *et al.*, 1998), which is bound by the ~70-amino-acid, N-terminal domain in human CBS (hCBS) (Meier *et al.,* 2001). In contrast, CBS from yeast (*Saccharomyces cervisiae*) and *Trypanosoma cruzi* lacks the N-terminal domain of hCBS and do not bind heme (Jhee *et al.*, 2000; MacLean *et al.*, 2000; Nozaki *et al.*, 2001).

Purification of hCBS from mammalian tissues is complicated by its susceptibility to proteolysis and tendency to aggregate (Kraus and Rosenberg, 1983). Therefore, recombinant systems were developed for the expression of hCBS in *Escherichia coli.* For example, Kraus, *et al.* (1994) developed a system, in which hCBS was expressed in conjunction with the fusion partner β-galactosidase (β-gal), that yielded 8 mg/L of hCBS following purification with diethylaminoethyl (DEAE) cellulose ion exchange chromatography. Although premature *in vivo* proteolysis of the β-gal/hCBS fusion protein was observed (Frank *et al.*, 2007), making it difficult to employ the chromatography to purify hCBS and reducing the final yield, this system has been employed for the characterization of hCBS (Kraus *et al.,* 1994). An alternative *E. coli* expression system was developed in 1998 by Shan and Kruger, in which hCBS is expressed in conjunction with the fusion partner glutathione-*S*-transferase (GST) (Shan and Kruger, 1998). A yield of 0.5 mg/L was obtained using the GST/hCBS expression system. However, a disadvantage of

this system is that the glutathione sepharose chromatography resin is costly. Additionally, both of the aforementioned expression systems share a requirement for protease cleavage to remove the β-gal or GST fusion partner, followed by an additional purification step. Recently, a modified GST-hCBS expression construct was reported, which reduced the tag remaining at the N-terminus of hCBS, following proteolytic cleavage, to a single amino acid (Frank *et al.*, 2007). However, relying on fusion proteins for purification is less advantageous to simply tagging the protein as the fusion may interfere with protein function, despite the fact that the fusion protein can be proteolytically cleaved. The fusion may also cause misfolding prior to cleavage. These problems can be circumvented by the use of smaller affinity tags (Frank *et al.*, 2007).

A 6-His tag, enabling Ni-nitrilo triacetic acid (Ni-NTA) affinity chromatography, was incorporated in a series of hCBS expression constructs: (i) 6-His-GST/hCBS, (ii) 6-His-GFP/hCBS and (iii) 6-His-hCBS. Ni-NTA affinity chromatography was chosen because the resin is easily regenerated and is significantly less costly than glutathione sepharose. It is also more economical to use, as imidazole is employed for elution rather than the glutathione used to elute GST-tagged proteins from glutathione-based affinity resin. The yield and steady state kinetic parameters of hCBS expressed using the three different constructs were compared and 6-His/hCBS was found to be optimal. The continuous CBS assay developed by Aitken and Kirsch (2003) was employed for the first time to characterize hCBS and revealed previously unreported substrate inhibition by L-Hcys.

3.2. MATERIALS AND METHODS

3.2.1. Reagents

δ-Aminolevulinic acid (δ-ALA), L-lactate dehydrogenase (LDH), β-nicotinamide adenine dinucleotide (β-NADH, reduced form), Tris-HCl, thrombin, dithiothreitol (DTT), isopropyl β-D-1-thiogalactopyranoside (IPTG), DNase I, lysozyme, L-Ser and L-Hcys thiolactone were purchased from Sigma-Aldrich Inc (Sigma-Aldrich, St. Louis, MO). L-Hcys was prepared from the thiolactone via the method described by Kashiwamata and Greenberg (1970). Protease inhibitor tablets were a Roche product (Roche Ltd., Mississauga, ON). Nickel-nitrilotriacetic acid (Ni-NTA) resin was from Qiagen (Qiagen, Mississauga, ON) and 5, 5'-dithio-bis-(2-nitrobenzoic acid) (DTNB) was from Pierce (Pierce Biotechnology, Inc., Rockford, IL). Potassium phosphate (monobasic and dibasic) and imidazole were Fisher (Fisher Scientific Inc, Pittsburgh, PA) products. The 6-His-tagged cystathionine β-lyase (CBL) coupling enzyme, employed in the CBS assay, was expressed and purified as described previously (Aitken and Kirsch, 2003). Primers were synthesized by Integrated DNA Technologies Inc. (Coralville, IA). The pTrc99a/6-His-GST-hCBS construct was previously prepared by S. Aitken. Unless specified all the restriction enzymes were obtained from New England Biolabs (Ipswich, MA).

3.2.2. Preparation of the 6x-His/GFP-hCBS and 6x-His/hCBS Expression Construct

The plasmid selected for expression of the hCBS gene is pTrc99a. To facilitate the expression and subsequent purification of the protein, a fusion partner, enhanced green fluorescence protein-1 (eGFP-1), was inserted into the expression vector. The *eGFP-1*

gene was amplified from the pEGFP-1 plasmid using the GFP-Fc-*Nco*I-His (5'-TAG ACC ATG GCG CAT CAT CAC CAT CAC CAT ATG GTG AGC AAG GGC GAG-3') and GFP-Rc-*Kpn*I (5'-GGC ATG GAC GAG CTG TAC AAG TAA-3') primers. A 6-His tag was incorporated at the N-terminus of eGFP-1 (in the GFP-Fc-*Nco*I-His primer) to enable affinity protein purification using Ni-NTA chromatography. The amplified eGFP-1 gene was subsequently directionally inserted between the *Nco*I and *Kpn*I sites of multiple cloning site of pTrc99a plasmid.

In order to enable removal of the eGFP-1 fusion partner, *via* proteolytic cleavage, the pTrc99a-GFP construct was engineered to incorporate a linker sequence at the 3' end of the eGFP-1 gene. The nucleotide sequence of the linker was designed with flanking *Kpn*I sites, for insertion at the *Kpn*I site at the 3' end of the eGFP-1 gene, to enable conservation of the largest number of unique restriction sites in the multiple cloning site of the vector. As a result, insertion of the linker was non-directional, thereby necessitating screening to select a construct in which a single copy of the linker had been incorporated in the correct orientation. The linker was designed to incorporate a *Spe*I restriction site such that digestion with *Spe*I endonuclease, followed by re-ligation of the vector, would enable selection of a construct containing a single copy of the linker. The *Spe*I restriction site is unique in the linker and does not occur in the plasmid and eGFP-1 sequences. The presence and orientation of the linker sequence was also confirmed by diagnostic polymerase chain reaction (PCR) using interior verification primers from the linker sequence and the eGFP-1 gene. The final step in the engineering of the pTrc99a-GFP-linker vector, prior to insertion of the hCBS gene, was modification of two restriction sites. The *Kpn*I site, at the 3' end of the linker, was converted to a *Nde*I site by whole plasmid

mutagenic PCR (Galas *et al.,* 1989) using the pTrc-KpnI-NdeIf-2 (5'-CTG GTG CCA CGC GGT AGT CAT ATG CGG GGA TCC TCT AGA GTC GAC-3') and pTrc-KpnI-NdeIr-2 (5'-GTC GAC TCT AGA GGA TCC CCG CAT ATG ACT ACC GCG TGG CAC CAG-3') primers. The pTrc99a vector contains a *Nde*I site, outside of the multiple cloning site. Therefore, to produce a final construct (pTrc99a-GFP-linker) with a unique *Nde*I site, immediately 3' of the linker sequence, for insertion of the hCBS gene, whole plasmid mutagenic PCR was employed, using the pTrc-*Nde*I-*BglII*f (5'-GTA TTT CAC ACC GAG ATC TGTGCACTC TCAGT ACAA TCTG-3') and pTrc-*Nde*I-*Bgl*IIr (5'-CAG ATT GTA CTG AGA GTG CAC AGA TCT CGG TGT GAA ATAC-3') primers, to convert this additional *Nde*I site to a *Bgl*II site. The hCBS gene was amplified from a vector containing the full-length gene (pGEX4T1/hCBS) using the hCBS-Fc-NdeI (5'-GAC AAA CAT ATG CCT TCT GAG ACC CCC C-3') and hCBS-Rc-SalI (5'-GGA TCC GAT CGA CTT CAC TTC TGG TCC CGC-3') primers. The pTrc99a/GFP-linker vector constructed contains unintentional *Nde*I site between the last codon (CAT) of the 6x-His tag and the start codon (ATG) of GFP. Since digestion of 6-His/GFP vector using *NdeI*/*Sal*I will remove the GFP-linker component of the construct leaving only the 6x-His tag, insertion of hCBS amplicon into these sites produced the plasmid construct for pTrc99a/6-His-hCBS. The correct ligation of hCBS into the *NdeI*/*Sal*I site was verified by PCR. To create the GFP-linker-hCBS portion of the engineered expression construct the unintentional *Nde*I site between 6-His tag and GFP was changed in to *Bmt*I using a forward mutagenesis primer *Nco*I-HisGFP-*Bmt*Ib (5'-CAG ACC ATG GCG CAT CAT CAC CAT CAT CAC GCT AGC GTG AGC AAG GG–3') so that subsequent digestion with *NdeI*/*Sal*I will allow insertion

of hCBS amplicon. This construct was also sequenced to ensure correct insertion and orientation, as well as the lack of mutations, in each component.

3.2.3. Protein Expression

The 6-His/hCBS, 6-His-GFP/hCBS and 6-His-GST/hCBS constructs were expressed and purified using the same protocol. A 100-mL, overnight culture of *E. coli* strain DH10b (Amersham) containing the hCBS construct in the high copy expression plasmid pTrc-99a was grown in rich media (12 g/L tryptone, 24 g/L yeast extract, 6.3 g/L glycerol, 12.5 g/L dibasic potassium phosphate, 3.8 g/L monobasic potassium phosphate) containing 20 mL/L of 50X Vogel Bonner salt solution (2.87 M K_2HPO_4, 0.041 M $MgSO_4.7H_2O$, 0.48 M citric acid (anhydrous), 0.84 $NaNH_4PO_4.4H_2O$) (Vogel and Bonner, 1956), 75mg/L δ-aminolevulinic acid (δ-ALA) and 100 μg/mL ampicillin. Three liters of rich media were inoculated with the overnight culture media (at a 1:50 inoculant-to-media ratio) in baffled, 2.8-L Fernbach flasks (1 L per flask). Cells were grown at 30°C in a shaking incubator (approximately 200 rpm) until the OD_{600} reached 0.5. At this point IPTG was added to a final concentration of 0.2 mM and the cells were grown for an additional 16 hours. The cells were harvested by centrifugation at 4000 rpm for 10 minutes at 4°C and the cell pellets were washed by resuspensing in 100 mL of 0.85% NaCl followed by centrifugation at 4000 rpm for 10 minutes. Cell pellets were resuspended in 40 mL of lysis buffer (50 mM potassium phosphate, pH 7.8, 10 mM imidazole, 20 μM PLP), containing one "EDTA-free" protease inhibitor tablet (Roche), prior to the addition of lysozyme (1 mg/mL) and DNase I (10 μg/mL). The resuspended cells were incubated at room temperature for 20 minutes, to allow digestion of the cell wall and DNA by lysozyme and DNase I,

respectively, before being further disrupted by sonication (8 cycles of 30 sec at 50% duty cycle; Vibra Cell sonicator, Sonic and Material, Inc.). The cell lysate was centrifuged at 15000 rpm for 45 minutes at 4°C to remove cell debris and the supernatant was loaded on a ~10-mL Ni-nitrilo triacetic acid (Ni-NTA) column, equilibrated with lysis buffer. The column was subsequently washed with 10 column volumes of lysis buffer and the protein was eluted with a 200-mL linear gradient of 10-200 mM imidazole in lysis buffer. Aliquots (20 μL) of each of the collected fractions (approximately 4 mL) were mixed with an equal volume of 2X protein loading buffer (100 mM Tris-HCl (pH 8), 4% SDS, 20% glycerol, 0.2% bromphenol blue and 200 mM dithiothreitol), heated for 3 minutes at 95°C to denature the protein, and analyzed by SDS-PAGE. Fractions containing pure hCBS protein were pooled, concentrated and dialyzed overnight in storage buffer (50 mM potassium phosphate buffer, 20 μM PLP, and 1mM EDTA). Glycerol was added to 20 % (v/v) and samples were aliquoted and stored at -80°C. The protein concentration was determined by the Bradford method (BioRad), using bovine serum albumin (BSA) as a standard (Bradford, 1976). The purified 6-His-GST/hCBS and 6-His-GFP/hCBS proteins were treated with thrombin to remove the fusion partner. The protein was incubated for 6 hrs with 10 units of thrombin (Sigma-Aldrich) per mg of hCBS fusion protein in protease buffer (140 mM NaCl, 2.7 mM KCl, 10 mMNa_2HPO_4, 1.8 mM KH_2PO_4, pH 7.3). The cleavage products were separated *via* Ni-NTA chromatography.

3.2.4. Enzyme Assays

Enzyme activity was measured in a total volume of 100 μL at 25°C with a Spectramax 340^{384PC} (Molecular Devices, Sunnyvale, CA) spectrophotometer. The assay

buffer comprised 50 mM Tris (pH 8.6) and 20 μM PLP. A background rate, for all components except the hCBS enzyme, was recorded for each sample before initiating the reaction by the addition of hCBS. Data was fit by nonlinear regression with SAS (SAS Institute, Cary, NC).

The reverse-physiological hydrolysis of L-Cth to L-Ser and L-Hcys by hCBS was detected *via* the reaction of 5, 5'-dithiobis-(2-nitrobenzoic acid) (DTNB) with the free thiol of the L-Hcys product, releasing the TNB thiolate ion, which absorbs at 412 nm (Ellman, 1959; Yamagata *et al.*, 1993; Aitken and Kirsch, 2003). Reactions were carried out in assay buffer containing 2 mM DTNB and 0.044 – 25.0 mM L-Cth. Absorbance changes were monitored at 412 nm ($\Delta\varepsilon_{412}$ = 13 600 $M^{-1}cm^{-1}$). Michaelis-Menten plots were fit to the data (equation 1) to determine the kinetic parameters k_{catR} and $K_m^{L\text{-}Cth}$. The value of $k_{catR}/K_m^{L\text{-}Cth}$ was obtained independently from equation 2 (Aitken and Kirsch, 2003).

$$\frac{v}{[E]} = \frac{k_{cat} \times [L-Cth]}{K_m + [L-Cth]} \qquad \text{(equation. 1)}$$

$$\frac{v}{[E]} = \frac{k_{cat}/K_m \times [L-Cth]}{1 + [L-Cth]/K_m} \qquad \text{(equation. 2)}$$

The CBS-catalyzed condensation of L-Ser and L-Hcys to produce L-Cth was assayed *via* a continuous assay that is reliant on the coupling enzymes cystathionine β-lyase (CBL) and lactate dehydrogenase (LDH) (Aitken and Kirsch, 2003). Optimal concentrations of 1.6 μM and 1.4 μM were determined for the CBL and LDH coupling enzymes, respectively, in the hCBS β-replacement assay. Reactions were carried out in assay buffer

containing 1.5 mM NADH. The concentration range of 0.1 mM – 12 mM for L-Hcys , and 0.5 mM – 20 mM for L-Ser substrates were employed. Reactions were initiated by the addition of hCBS and the conversion of NADH to NAD^+ was monitored at 340 nm ($\Delta\varepsilon_{340}$ = 6200 $M^{-1}cm^{-1}$). The linear range, over which activity observed is proportional to hCBS enzyme concentration, was determined for hCBS (Aitken and Kirsch, 2003). The values of the full set of kinetic parameters for the condensation reaction were determined from the global fit of the data to equations 4, in which k_{catF} is the turnover number for the condensation reaction, $K_m^{L\text{-}Hycs}$ and $K_m^{L\text{-}Ser}$ are the Michaelis constants for L-Hcys and L-Ser, respectively, and $K_{iF}^{L\text{-}Hcys}$ and is the inhibition constant of substrate inhibition by L-Hcys (Aitken and Kirsch, 2003).

$$\frac{v}{[E]} = \frac{k_{cat}[L-Ser][L-Hcys]}{K_m^{L-Hcys}[L-Ser] + K_m^{L-Ser}[L-Hcys] + [L-Ser][L-Hcys]} \qquad \text{(equation 3)}$$

$$\frac{v}{[E]} = \frac{k_{cat}[L-Ser][L-Hcys]}{K_m^{L-Hcys}[L-Ser] + K_m^{L-Ser}[L-Hcys]\left(1+\frac{[L-Hcys]}{K_{iF}^{L-Hcys}}\right) + [L-Ser][L-Hcys]} \qquad \text{(equation 4)}$$

3.3. RESULTS

3.3.1. Synthesis of the pTrc99a/GFP-hCBS construct

Introduction of the GFP gene and the linker into the pTrc99a vector was confirmed by diagnostic PCR and restriction digestion with *SpeI*/*Nco*I, which have restriction sites in the linker and the eGFP-1 gene, respectively (Figure 3.1). Sequencing of the construct provided final confirmation of correct insertion as well as a lack of other mutations or frame shifts. Similar verification procedures were used for the correct ligation of hCBS into the *NdeI*/*Sal*I site of the multiple cloning site of pTrc99a/GFP-linker construct (Figure 3.2).

3.3.2. Evaluation of the Three hCBS Constructs

Three constructs were compared in an attempt to create a robust and convenient *E. coli* expression system for hCBS that would allow Ni-NTA affinity chromatography to be employed for purification. These constructs all include an N-terminal, 6-His tag, but differ in the presence or nature of the fusion partner: (i) 6-His-GST/hCBS, (ii) 6-His-GFP/hCBS and (iii) 6-His/hCBS. An observable feature of hCBS expression is that *E. coli* cell pellets are brown, due to the presence of the heme cofactor in hCBS. This allows visual inspection to be employed as a preliminary estimate of the efficiency of hCBS expression and a dark brown color was observed on expression of the 6-His/hCBS construct, in comparison with the 6-His-GST/hCBS and 6-His-GFP/hCBS constructs.

Table 3.1. Primer combinations employed in verification of the pTrc99a/6-His-GFP/hCBS construct.

Primer combination	Purpose of PCR	Size of DNA amplified (base pair)	Expected size of amplicon (base pair)
pSECseq0 and Linker.IntR.	Linker ligation verification	~1100	1150
Linker. IntR. and GFP. IntF	Verification for proper eGFP-1 and linker ligation	~350	375
GFP. IntF. and PSECseq7r	Verification for proper eGFP-1 and linker ligation	~750	780
PSECseq0 and GFP. IntR	Verifying the ligation of eGFP-1	~800	805
NcoI-His-eGFP-1 and Linker.IntR.	Verifying the existence of the linker on the 3' end of eGFP-1	~800	790
hCBS seq2 and PSECseq7r	hCBS ligation verification right next to the 3' end of the linker	~1300	1345
hCBS seq4 and PSECseq7r	hCBS ligation verification next to the 3' end of the linker	~600	630

Figure 3.1. Diagnostic restriction digestion and PCR reactions conducted for verification of pTrc99a/GFP-linker construct. (**A**) Schematic representation of the primers and restriction sites used in the linker verification procedures. Solid directional arrows indicate region of primer sites and broken arrows indicate restriction sites used (*Nco*I at the 5' end of GFP and *Spe*I at the middle of the linker). Primers: i = pSECseq0 (in the vector, 300 bp 5' of GFP), ii = GFP-intF (~300bp 3' of the start codon of GFP), iii = Linker-intR (internal linker primer, ~30bp from the 5' end), and iv = pSECseq7r (in the vector, ~400 bp 3' of the linker). Drawings are not to scale. (**B**) PCR verification of ligation of linker to the 3'-end of eGFP-1 in pTrc99a-GFP construct. The PCR primer combinations are: **Lane 1** = 1Kb DNA ladder in base pairs; **Lane 2** = linker intR. and GFP IntF (~350bp); **Lane 3** = Linker IntR. and pseq.0 (~1100bp); **Lane 4** = GFP IntF. and Pseq7r (~750bp). (**C**) Digestion of pTrc99a-GFP construct from 4 transformants with *Spe*I and *Nco*I restriction endonucleases Only clones 1, 2 and 4 show the ~750-bp band expected.

A


i
ii
iii
iv
pTrc-99A
GFP
Linker
pTrc-99a

B

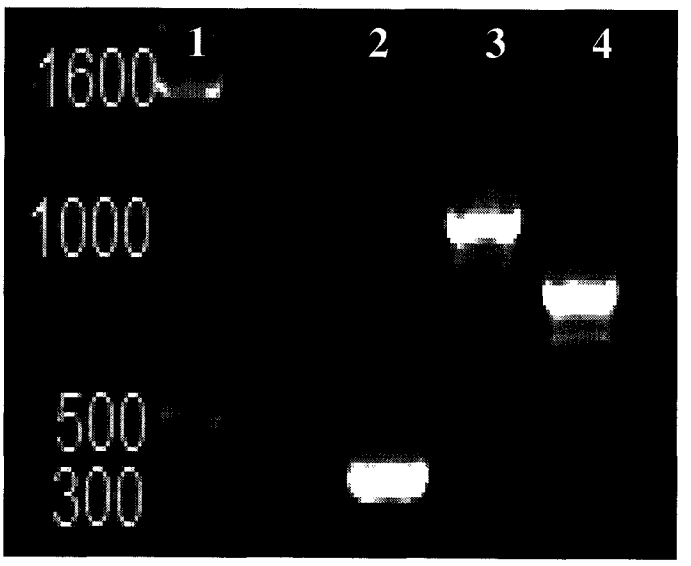
1
2
3
4
1600
1000
500
300

C

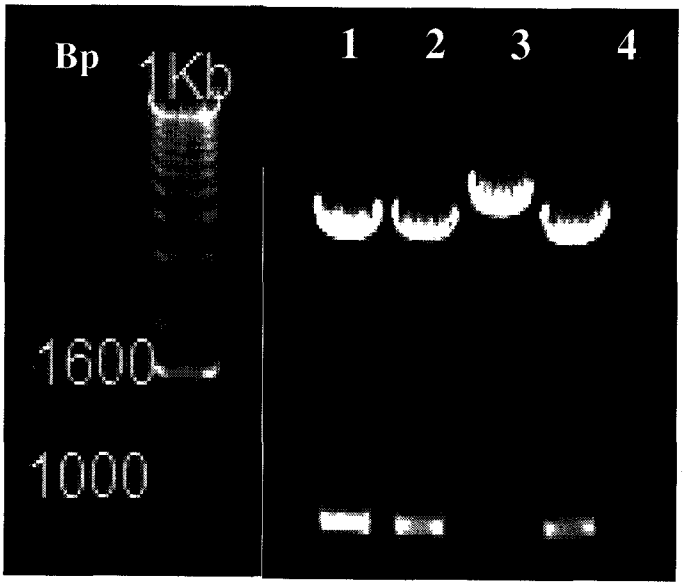
Bp
1Kb
1
2
3
4
1600
1000

Figure 3.2. Verification of pTrc99a/GFP-hCBS construct. (**A**) Schematic representation of the primers and restriction sites used in the verification procedure. Primers i-iv are described in the legend of figure 3.1. A pair of primers in the hCBS gene (***v*** = hCBSseq2 and ***vi*** = hCBSseq4) were also employed here. Drawings are not to scale. (**B**) Agarose gel of diagnostic PCR reactions. Lanes are defined as follows: **Lane 1** = 1Kb DNA ladder; **Lanes 3 - 7** are the PCR products (Table 3.1) of the (**3**) PSECseq0 and GFPintR. primers (~800bp); (**4 and 5**) the *Nco*I-His-eGFP-1 and Linker-IntR primers (~800bp); (**6**) the hCBS-seq2 and PSECseq7r primers (~1300bp); (**7**) is the hCBS-seq4 and pSECseq7r primers (~600bp).

A

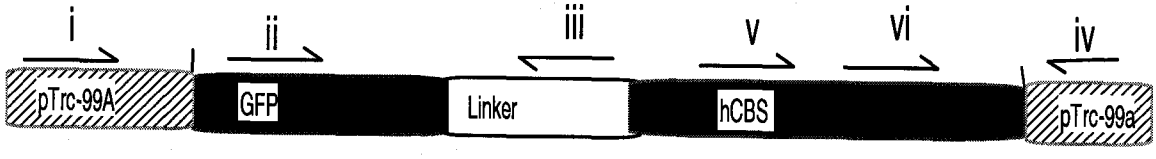
i
ii
iii
v
vi
iv
pTrc-99A
GFP
Linker
hCBS
pTrc-99a

B

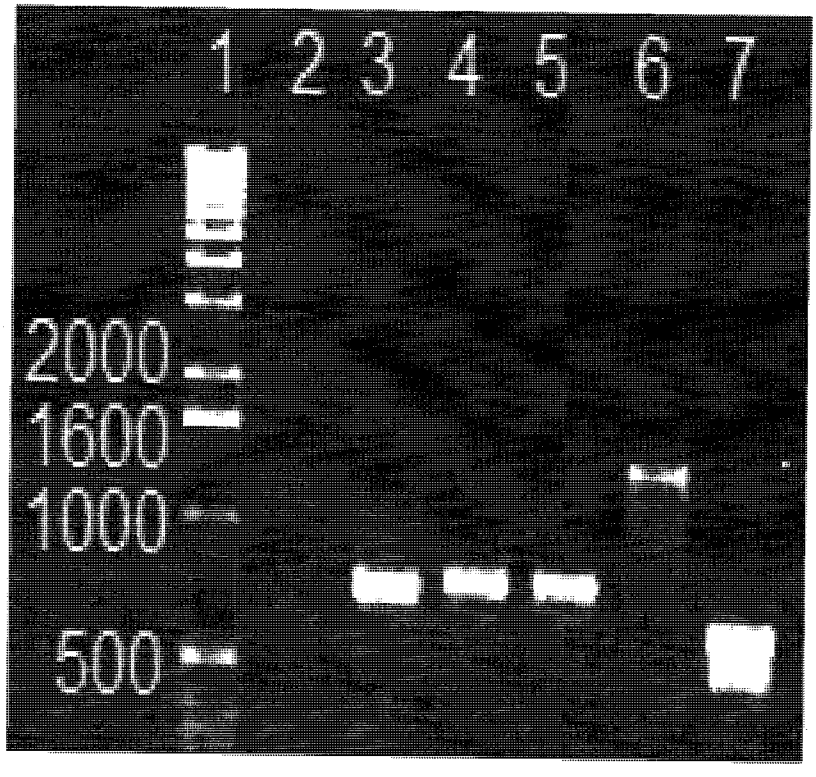
1 2 3 4 5 6 7
2000
1600
1000
500

Purification of 6-His-GST/hCBS *via* Ni-NTA chromatography yielded protein of only approximately 50% purity (Figure 3.3A). Thrombin treatment of the protein produced the expected 26 and 63 kDa bands, corresponding to GST and hCBS, respectively, while the 90-kDa band of the fusion protein was not observed, demonstrating that protease cleavage was successful (Figure 3.3B). In contrast with 6-His-GST/hCBS, purification of 6-His-GFP/hCBS yielded protein of >80% purity (Figure 3.4A). Thrombin treatment of the protein produced the expected 27 and 63 kDa bands, corresponding to GFP and hCBS, respectively, while the 90-kDa band of the fusion protein was not observed, demonstrating that protease cleavage was successful (Figure 3.4B). Of the three constructs, 6-His/hCBS was the most pure following Ni-NTA chromatography, as demonstrated by SDS-PAGE (Figure 3.5).

The 6-His/hCBS (Figure 3.5) and thrombin-cleaved hCBS from the GST (Figure 3.3B) and GFP (Figure 3.4B) fusion proteins were assayed using the continuous CBS assay (Aitken and Kirsch, 2003). Comparison of the kinetic parameters (Table 3.2.) demonstrates that the k_{cat}/K_m of 6-His/hCBS for both substrates was approximately 10-fold higher than that of the other two enzymes. This is due in part to its greater purity. The graphs of activity versus L-Hcys concentration clearly indicate substrate inhibition of hCBS (Figure 3.6).

Figure 3.3. (**A**) SDS-PAGE of fractions from purification of 6-His-GST/hCBS by Ni-NTA chromatography. **Lane 1:** protein ladder; **Lanes 2-12:** every third fraction starting from the 13^{th} fraction. (**B**) Analysis of the thrombin-cleavage products of 6-His-GST/hCBS. **Lane M:** protein ladder; **Lane 1:** 6-His/GST-hCBS before cleavage, **Lane 2:** following 5 hours of cleavage and **Lane 3:** following cleavage overnight at 16°C and purification with Ni-NTA.

A

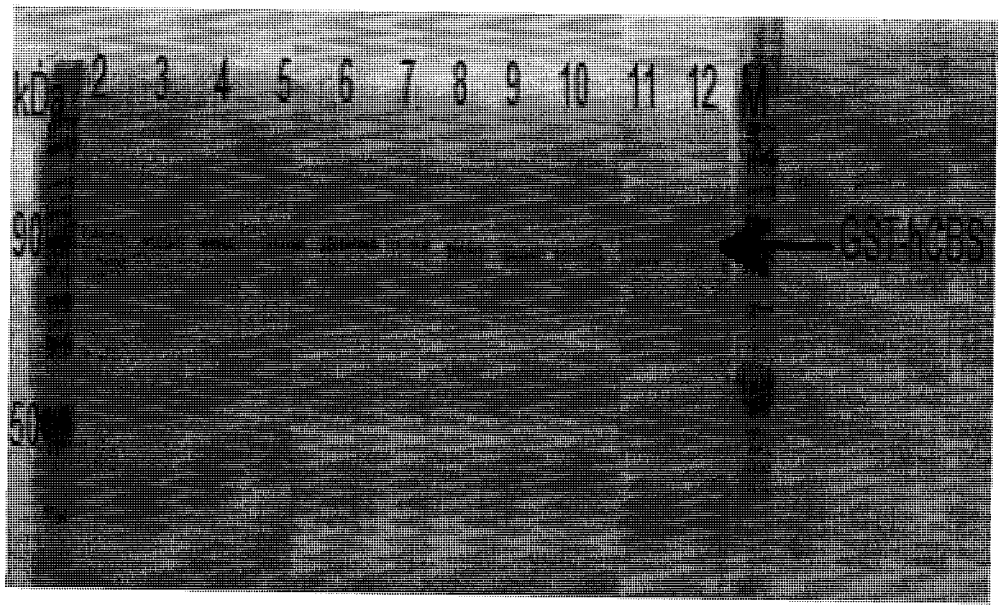

B

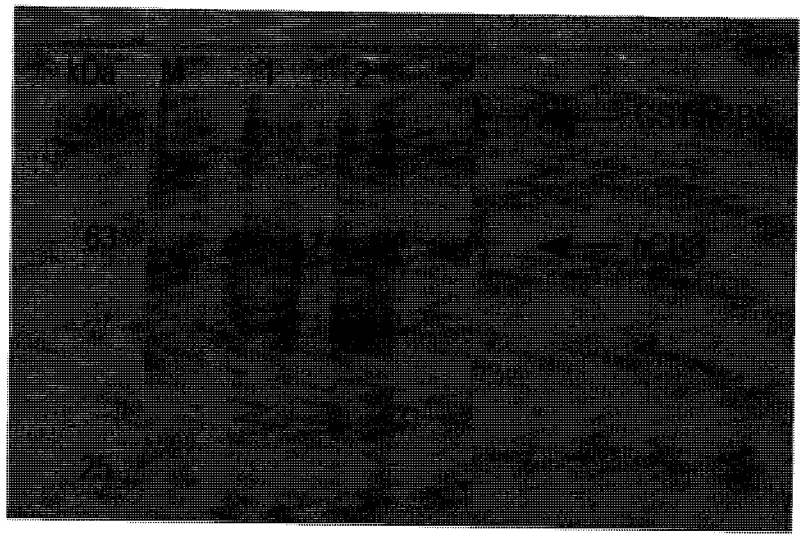

Figure 3.4. (**A**) SDS-PAGE of fractions from purification of 6-His-GFP/hCBS by Ni-NTA chromatography. **Lane 1:** protein ladder; **lanes 2-12:** every third fraction starting from the 13^{th} fraction. (**B**) Analysis of the thrombin-cleavage products of 6-His-GFP/hCBS. **Lane M:** protein ladder; **lane 1:** 6-His/GFP-hCBS before cleavage, **lane 2:** following 5 hours of cleavage and **lane 3:** following cleavage overnight at 16°C and purification with Ni-NTA.

A

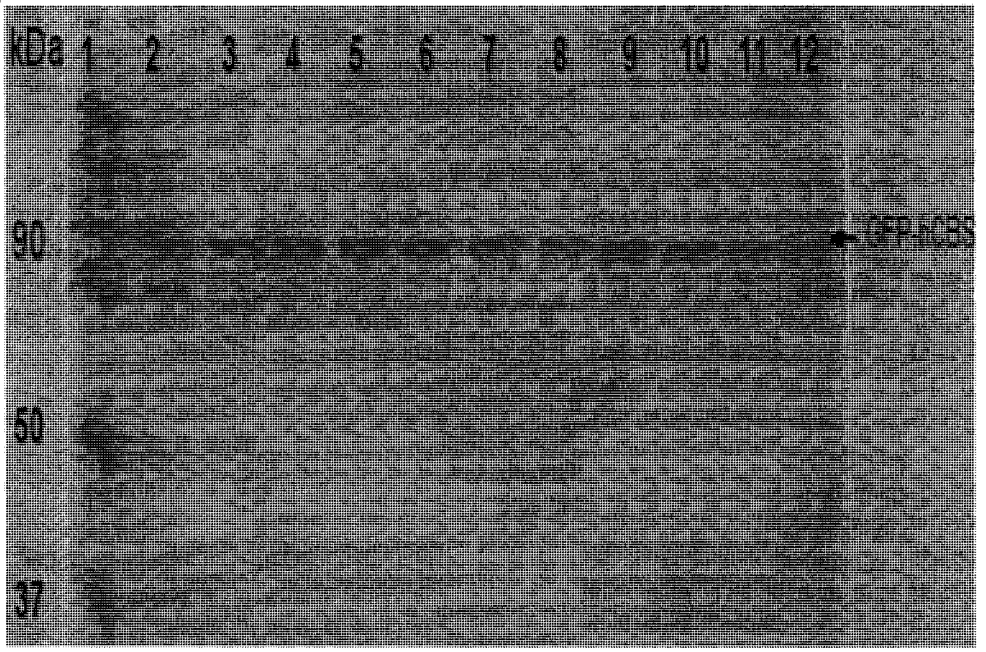
kDa 1 2 3 4 5 6 7 8 9 10 11 12
90
50
37
GFP-hCBS

B

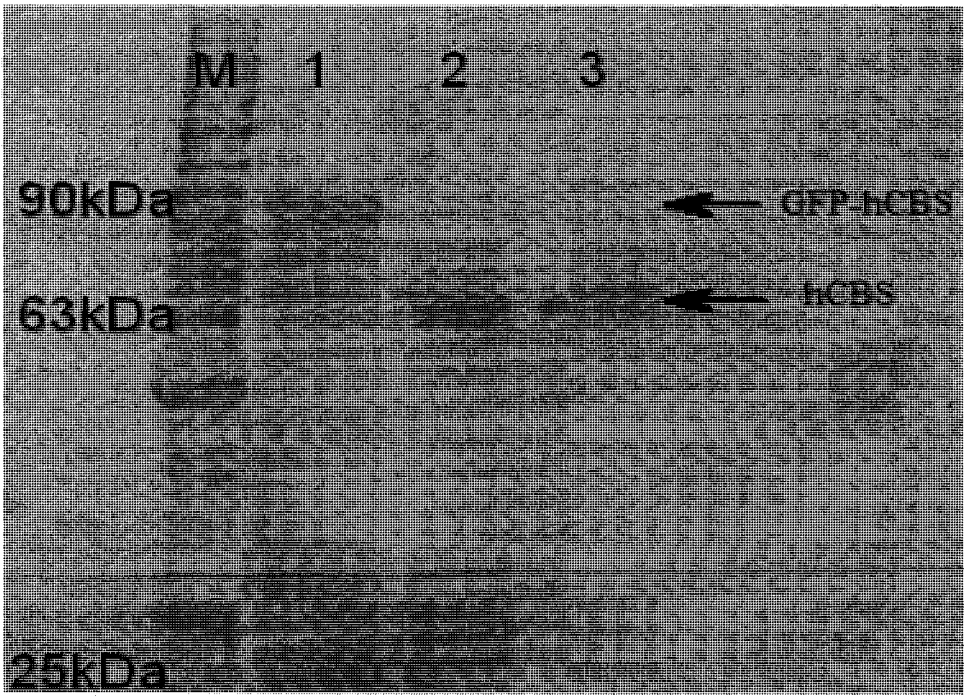
M 1 2 3
90kDa
63kDa
25kDa
GFP-hCBS
hCBS

Figure 3.5. SDS-PAGE of fractions from purification of 6-His-hCBS by Ni-NTA chromatography. **Lane 1:** protein ladder; **Lanes 2-12:** every third fraction starting from the 13^{th} fraction.

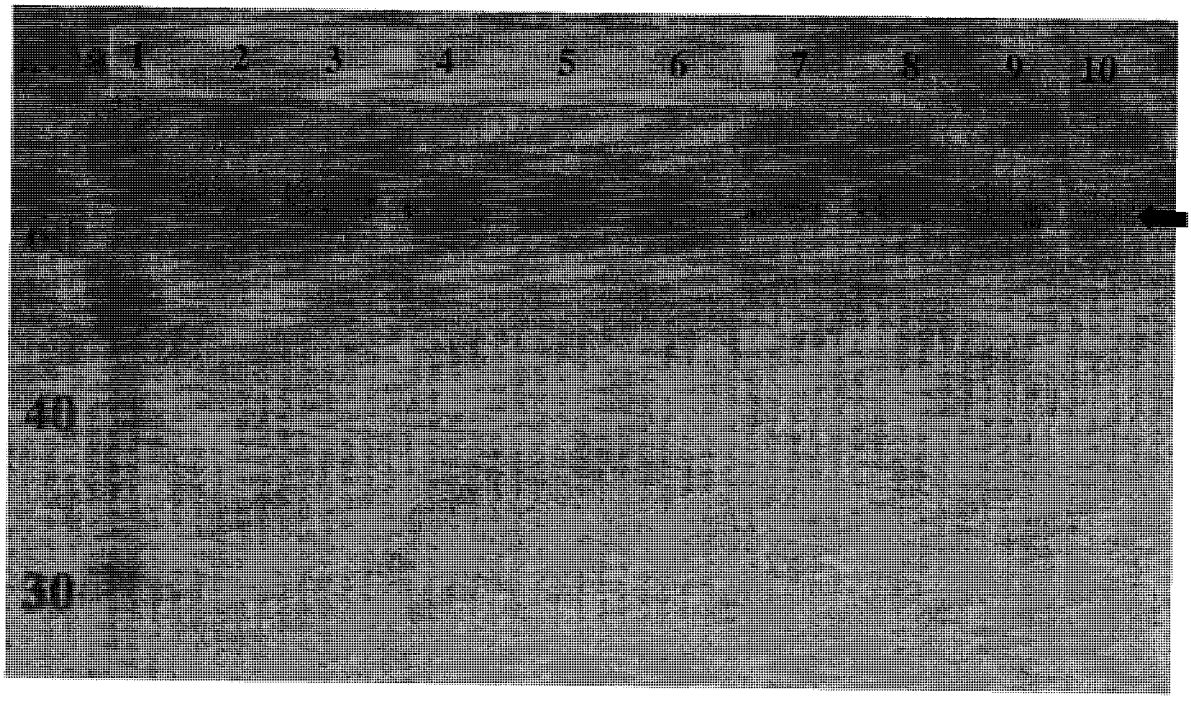
1
2
3
4
5
6
7
8
9
10
40
30
6x-His
hCBS

3.3.3. Characterization of hCBS

Analysis of the plots of 6-His/hCBS activity versus L-Hcys concentration 0.2-30 mM L-Ser (Figure 3.7) demonstrates mild substrate inhibition by L-Hcys. Therefore, for the global fit equation 3 was modified to incorporate a substrate inhibition term ($K_{iF}^{L\text{-}Hcys}$), producing equation 4 (Aitken and Kirsch, 2003; Jhee *et al.*, 2000). The ability of 6-His/hCBS to catalyze the hydrolysis of L-Cth, producing L-Ser and L-Hcys, was measured by Pratik Lodha. The kinetic parameters for the physiological, condensation reaction, as well as the L-Cth hydrolysis reaction are provided in Table 3.3.

Figure 3.6. Michaelis-Menten plots of hCBS activity at (**A**, **C** and **E**) 0.5-20 mM L-Ser and (**B**, **D** and **F**) 0.1-12 mM L-Hcys at fixed concentrations of 2 mM L-Hcys and 12 mM L-Ser, respectively, for (**A** and **B**) 6-His-hCBS (**C** and **D**) 6-His-GST/hCBS following thrombin cleavage and (**E** and **F**) 6-His-GFP/hCBS following thrombin cleavage Conditions: 50 mM Tris (pH 8.6), 20 μM PLP, 1.5 mM NADH, 1.6 μM CBL, 1.4 μM LDH and 1.76 μM hCBS.

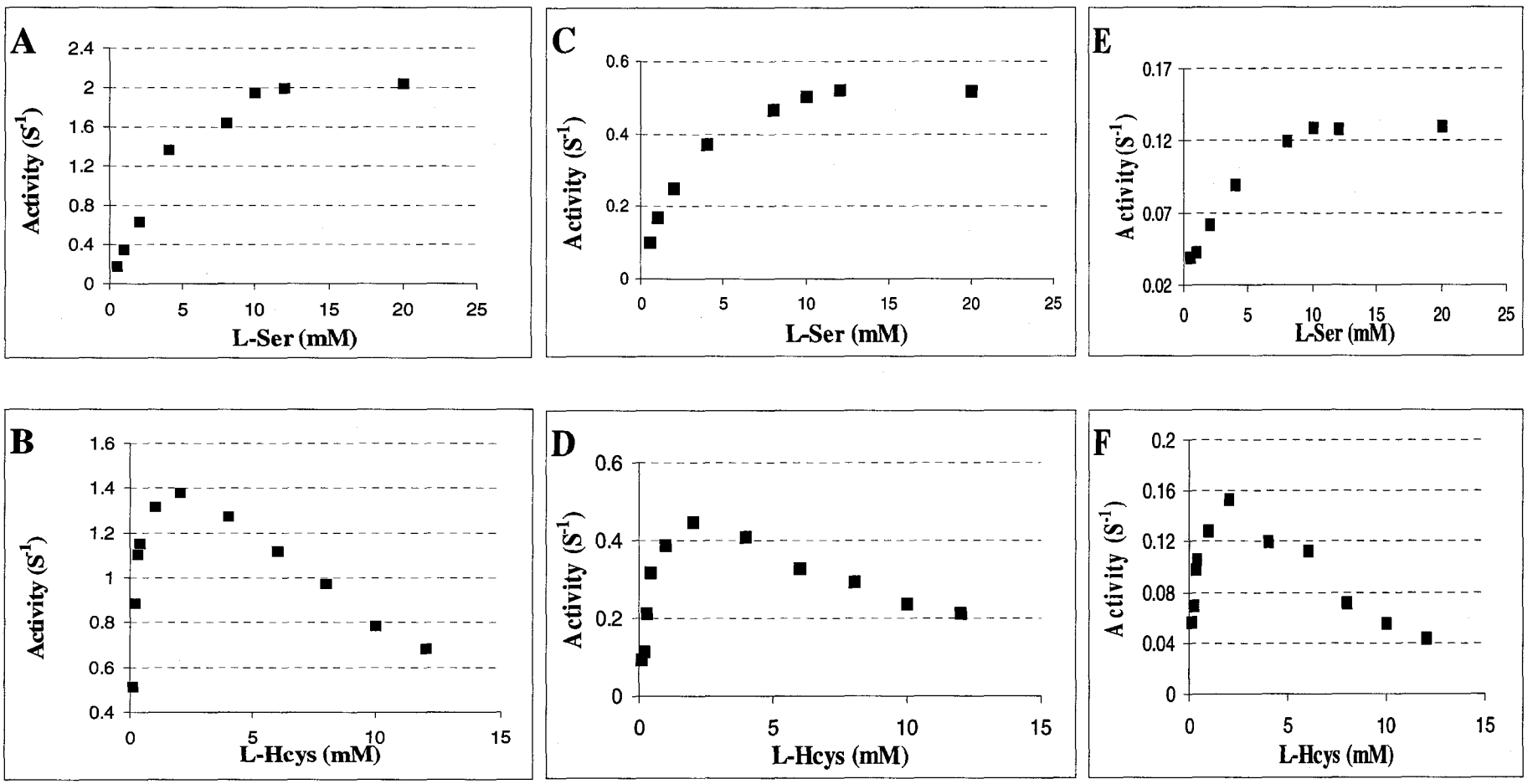
A
Activity (S^{-1})
2.4
2
1.6
1.2
0.8
0.4
0
0 5 10 15 20 25
L-Ser (mM)
C
Activity (S^{-1})
0.6
0.4
0.2
0
0 5 10 15 20 25
L-Ser (mM)
E
Activity (S^{-1})
0.17
0.12
0.07
0.02
0 5 10 15 20 25
L-Ser (mM)
B
Activity (S^{-1})
1.6
1.4
1.2
1
0.8
0.6
0.4
0 5 10 15
L-Hcys (mM)
D
Activity (S^{-1})
0.6
0.4
0.2
0
0 5 10 15
L-Hcys (mM)
F
Activity (S^{-1})
0.2
0.16
0.12
0.08
0.04
0
0 5 10 15
L-Hcys (mM)

Table 3.2. Comparison of the kinetic parameters of hCBS purified, and thrombin-cleaved where necessary, from the 6-His-GST/hCBS, 6-His-GFP/hCBS and 6-His/hCBS expression systems.

Kinetic Parameters[a,b]	**hCBS from GST tag**	**hCBS from GFP tag**	**6-His/hCBS**
$K_{cat}^{L\text{-}Ser}$ (s^{-1})	0.6 ± 0.2	0.200± 0.008	2.7 ± 0.2
$K_{cat}^{L\text{-}Hcys}$ (s^{-1})	0.60 ± 0.07	0.200 ±0.008	1.5 ± 0.1
$K_m^{L\text{-}ser}$ (mM)	2.6 ± 0.3	2.4 ± 0.4	5 ± 1
$K_m^{L\text{-}Hcys}$ (mM)	0.5 ± 0.1	0.23± 0.03	0.14 ± 0.03
$K_{cat}^{L\text{-}Hcys}/K_m^{L\text{-}Hcys}$ ($mM^{-1}.s^{-1}$)	1.2 ± 0.2	0.73± 0.08	10 ± 1
$K_{cat}^{L\text{-}Ser}/K_m^{L\text{-}ser}$ ($mM^{-1}.s^{-1}$)	0.23 ± 0.02	0.060 ± 0.009	0.60 ± 0.09
hCBS yield (mg/L)	0.4	0.3	1.9

[a]Kinetic parameters determined from the fit of data to equations 1 and 2.

[b]Kinetic parameters were determined at 25°C

Figure 3.7. The effect of (**A**) [L-Ser] and (**B**) [L-Hcys] on the β-replacement activity of 6-His/hCBS. Conditions: 50 mM Tris (pH 8.6), 20 μM PLP, 1.5 mM NADH, 1.6 μM CBL, 1.4 μM LDH, 1.76 μM wt 6-His-hCBS 0.1-12 mM L-Hcys (0.1, 0.2, 0.3, 0.4, 0.7, 1, 2, 4, 6, 8, 10 and 12 mM) and0.2-30 mM L-Ser (0.2, 0.5, 1, 2, 4, 6, 8, 10, 12, 15, 20, and 30 mM).

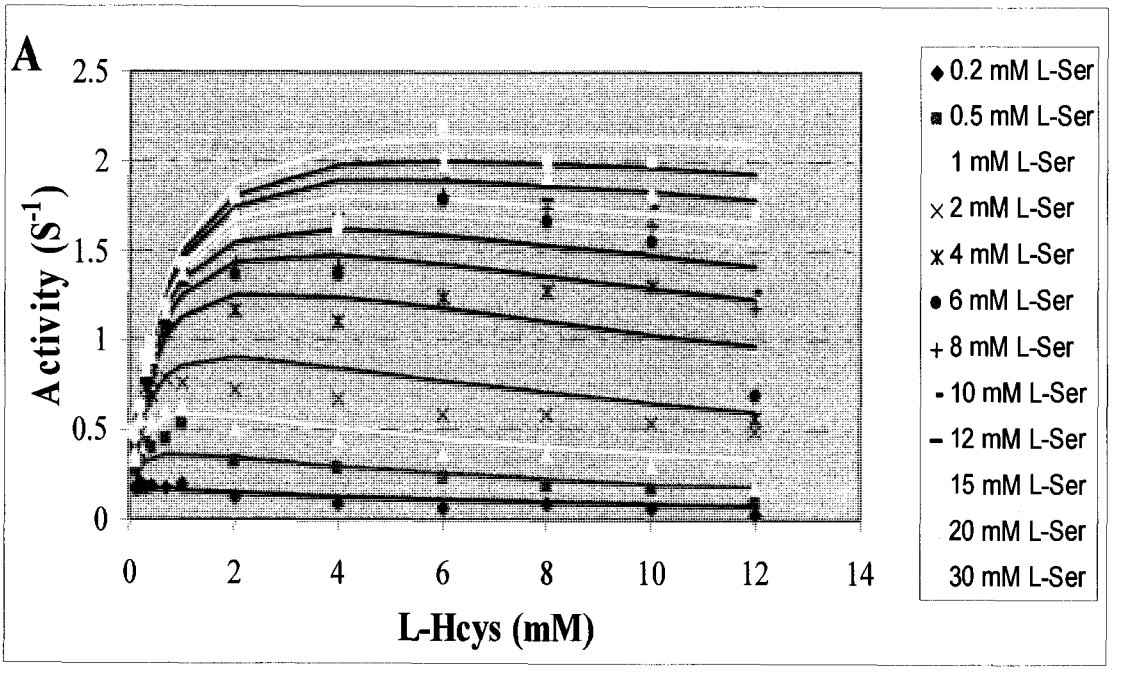
A
Activity (S^{-1})
2.5
2
1.5
1
0.5
0
0
2
4
6
8
10
12
14
L-Hcys (mM)
0.2 mM L-Ser
0.5 mM L-Ser
1 mM L-Ser
2 mM L-Ser
4 mM L-Ser
6 mM L-Ser
8 mM L-Ser
10 mM L-Ser
12 mM L-Ser
15 mM L-Ser
20 mM L-Ser
30 mM L-Ser

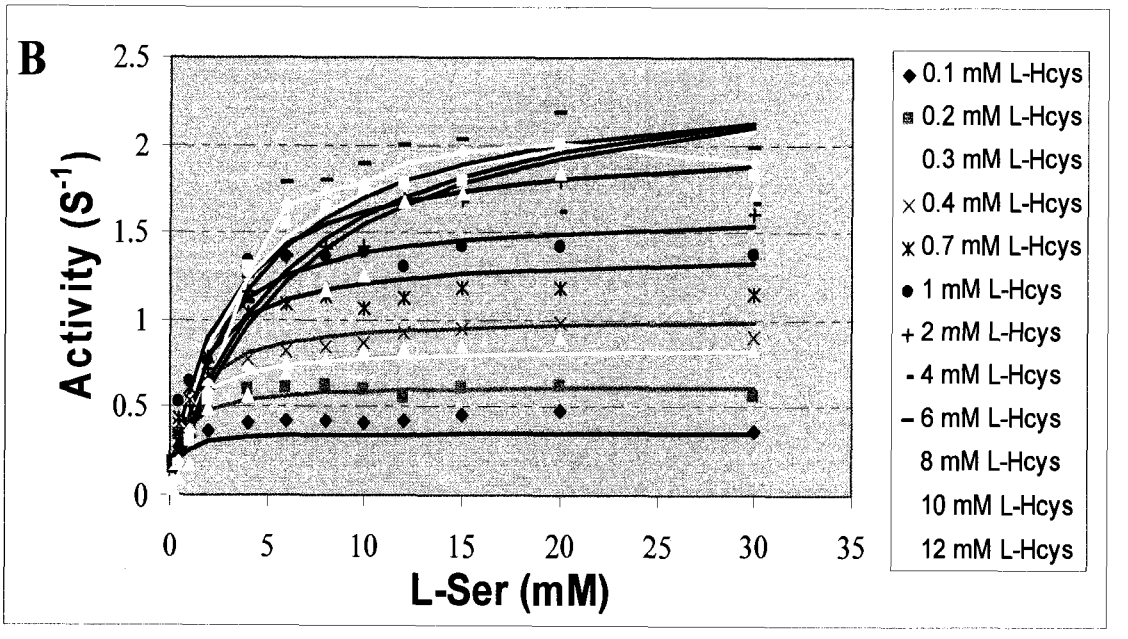
B
Activity (S^{-1})
2.5
2
1.5
1
0.5
0
0
5
10
15
20
25
30
35
L-Ser (mM)
0.1 mM L-Hcys
0.2 mM L-Hcys
0.3 mM L-Hcys
0.4 mM L-Hcys
0.7 mM L-Hcys
1 mM L-Hcys
2 mM L-Hcys
4 mM L-Hcys
6 mM L-Hcys
8 mM L-Hcys
10 mM L-Hcys
12 mM L-Hcys

Table 3.3. Steady state kinetic parameters of 6-His/hCBS.

Kinetic Parameter	
L-Ser + L-Hcys → L-Cth	
k_{cat} (s^{-1})	2.7 ± 0.1
$K_m^{L\text{-}Ser}$ (mM)	2.6 ± 0.3
$K_m^{L\text{-}Hcys}$ (mM)	0.66 ± 0.06
$k_{cat}/K_m^{L\text{-}Hcys}$ ($mM^{-1}s^{-1}$)	4.1 ± 0.1
$k_{cat}/K_m^{L\text{-}Sers}$ ($mM^{-1}s^{-1}$)	1.0 ± 0.1
$K_{iF}^{L\text{-}Hcys}$ (mM)	7.2 ± 1.6
L-Cth→ L-Ser+ L-Hcys	
k_{cat} (s^{-1})	0.090 ± 0.001
$K_m^{L\text{-}Cth}$ (mM)	0.04 ± 0.01
$k_{cat}/K_m^{L\text{-}Cth}$ ($mM^{-1}s^{-1}$)	2.1 ± 0.1

3.4. DISCUSSION

3.4.1. Evaluation of the Three hCBS Constructs

The purification of human cystathionine β-synthase (hCBS) from mammalian tissue is complicated by its tendency to aggregate and its susceptibility to proteolysis (Kraus and Rosenberg, 1983). Therefore, a recombinant expression system was developed, in which hCBS was expressed as a fusion protein with β-gal in *E. coli* (Kraus *et al.,* 1994). However, proteolytic cleavage within the *E. coli* host cells was observed during expression of the β-gal-hCBS construct, resulting in some loss of the fusion partner and reduced yield of hCBS purified *via* anion exchange chromatography (Kraus *et al.,* 1994). An alternative system, in which hCBS was expressed as a fusion protein with glutathione-*S*-transferase (GST) was also developed (Kruger and Shan, 1998). However, glutathione sepharose chromatography resin is expensive, the purified protein is susceptible to aggregation, likely due to the tetrameric structure of both GST and hCBS, and following thrombin cleavage of the GST-hCBS a 11-amino-acid tag remains attached to hCBS. Recently, a modified GST-hCBS expression construct was reported, which reduced the tag remaining at the N-terminus of hCBS, following proteolytic cleavage, to a single amino acid (Frank *et al.*, 2007). However, since this system relies on a large-fusion partner to facilitate purification, as those previously developed, the requirement for protease cleavage, which could be circumvented with a smaller tag, is maintained (Frank *et al.*, 2007).

A sequence encoding a 6-His tag was added to the N-terminus of the GST-hCBS coding sequence, producing the 6-His/GST-hCBS construct, with the goal of reducing the cost of purification (Qiagen; Sigma-Aldrich). However, although the 6-His/GST-hCBS

enzyme was isolated using Ni-NTA chromatography and thrombin cleavage was successful, (Figures 3.3B) the purity, yield and activity (Table 3.2) of hCBS produced in this manner were all approximately two-fold lower than reported by Kruger and Shan (1998). The GST fusion partner is a homotetrameric protein, which may compound the tendency of the homotetrameric hCBS enzyme to aggregate, thereby reducing yield. Therefore, a new expression system was developed to facilitate purification, minimize aggregation and reduce the length of the sequence remaining at the N-terminus of hCBS following proteolytic cleavage to remove the fusion partner. The soluble monomeric green fluorescent protein (GFP) (Yang *et al.*, 1996), the expression of which can be easily detected *in vivo* by its fluorescence (Chalfe *et al.*, 1994; Chalfe and Kain, 1996; Poppenborg *et al.*, 1997), was selected as a fusion partner for hCBS and the sequence of the linker between the GFP and hCBS proteins was designed to reduce the number of amino acids between the thrombin cleavage site and the N-terminus of hCBS. A 6-His tag was also added to the N-terminus of GFP to allow purification via Ni-NTA affinity chromatography. Purification of 6-His/GFP-hCBS and subsequent thrombin cleavage were successful (Figure 3.4B), but similar to the 6-His/GST-hCBS construct, activity was approximately two-fold lower (Table 3.2) than reported for GST-hCBS fusion constructs by Shan and Kruger (1998) and Frank *et al* (2007). A common step in purification of the GST-hCBS, 6-His/GST-hCBS and 6-His/GFP-hCBS constructs is proteolytic cleavage to release hCBS from its fusion partner. Given the size of the GST (26 kDa) and GFP (27 kDa) proteins, their removal is required prior to determination of kinetic parameters (Kraus and Rosenberg, 1983; Kruger and Shan, 1998, Frank *et al.*, 2007). This step requires incubation of the protein at room temperature for an extended period, which may reduce its

activity. Therefore, development of a purification procedure that eliminated the need for this step would reduce cost and the time required for purification, as well as minimizes loss of activity. A hCBS expression construct was designed in which only a N-terminal, 6-His tag was added to the hCBS coding sequence, in lieu of the β-gal, GST and GFP fusion partners employed to date, to enable Ni-NTA affinity chromatography. The resulting 6-His/hCBS construct yielded pure enzyme (Figure 3.5) with greater hCBS activity than the other constructs (Table 2.2) at a yield five-fold greater than the 6-His/GST-hCBS or 6-His/GFP-hCBS constructs and close to two-fold greater than that reported by Shan and Kruger for GST-hCBS (1998). This is the first time that recombinant hCBS has been expressed and purified with an affinity tag instead of a protein fusion partner. The k_{cat} of hCBS recovered from the modified GST-hCBS expression system described by Frank *et al.* (2007) was 3.67 s^{-1} which is nearly two-fold less than 6x-His/hCBS i.e. 6.48 (when corrected by a factor of 2.4 for temperature at 37°C) (Table 3.2).

3.4.2. Steady State Kinetic Characterization of hCBS from the Three Constructs

The CBS-catalyzed condensation of L-serine (L-Ser) and L-homocysteine (L-Hcys) to produce L-cystathionine (L-Cth) follows an ping pong mechanism. An endpoint assay, requiring separation and quantification of ^{14}C-labeled L-Cth product has been employed for the characterization of hCBS (Kraus, 1987). However, while this assay is sensitive, it allows accumulation of product, which may result in underestimation of k_{cat} and overestimation of $K_m^{L\text{-}Ser}$, as was observed for yeast CBS (Aitken and Kirsch, 2003). This assay is also time-consuming, which can lead to the acquisition of data sets of sub-optimal size. The continuous CBS assay, which relies on CBL and LDH as coupling enzymes, was

employed for the first time in this study to determine the steady state kinetic parameters of hCBS.

Reports of kinetic parameters for the forward condensation reaction by hCBS, (*i.e.* $k_{cat}^{L\text{-}Ser}$, $k_{cat}^{L\text{-}Hcys}$, $K_m^{L\text{-}Ser}$, and $K_m^{L\text{-}Hcys}$) showed a wide range of variations. For instance, reported values of $K_m^{L\text{-}Ser}$, $K_m^{L\text{-}Hcys}$ and k_{cat} range between 1.15 – 4.9 mM, 0.17 – 7.17 mM and 3.5 – 6.2 s^{-1}, respectively (Kraus *et al.,* 1978; 1994 1998; Frank *et al.*, 2007; Banerjee *et al.,* 1998; Janosik *et al.*, 2001; Kruger *et al.*, 2006). These discrepancies might be due to the lack of convenient expression system to reproducibly yield catalytically active protein or due to inaccuracy of the radioactive based endpoint assay.

The activity of hCBS following proteolytic cleavage from the 6-His/GST and 6-His/GFP fusion partners was reduced by approximately three-fold k_{cat} compared to 6-His/hCBS (Table 3.2). When corrected for temperature, the k_{cat} values of the 6-His/hCBS construct, determined at 25°C by saturating one substrate while varying the other, are within the standard error of the those reported at 37°C for hCBS purified from the modified GST-hCBS construct ($k_{cat}^{L\text{-}Hcys}$ = 4.66 ± 0.67 s^{-1} and $k_{cat}^{L\text{-}Ser}$ = 3.67 ± 0.67 s^{-1}) (Kraus *et al.,* 2007). Reports of the kinetic parameters of hCBS have always employed the method of saturating one substrate while varying the other due to the difficulty of the ^{14}C-L-Ser assay. Therefore, a full characterization of the 6-His/hCBS enzyme with the continuous assay was undertaken, in which both substrate concentrations were varied simultaneously and the entire data set was fit by global analysis to equation 4. Frank *et al.* (2007) determined the steady state kinetic parameters of hCBS, from the modified GST-hCBS construct, using the traditional radioactive based endpoint assay at 37°C, and reported $K_m^{L\text{-}Hcys}$ and $K_m^{L\text{-}Ser}$ values of 1.04 ± 0.24 mM and 1.41 ± 0.35 mM, respectively, and separate values of $k_{cat}^{L\text{-}}$

^{Hcys} and $k_{cat}^{L\text{-}Ser}$ of 4.66 ± 0.67 and 3.67 ± 0.67, respectively (Frank *et al.*, 2007). Comparison of these values to those determined in the full characterization of hCBS (Table 3.3) demonstrate a 1.6-fold reduction in $K_m^{L\text{-}Hcys}$ (0.66 ± 0.056 mM), a ~2-fold increase in $K_m^{L\text{-}Ser}$ (2.6 ± 0.33 mM) and a ~2-fold increase in k_{cat} (6.48 ± 0.098), when corrected 2.4-fold for the 12-degree temperature difference. Although the $K_m^{L\text{-}Ser}$ is greater than that reported by Frank *et al.* (2007), it is within the 1.15 – 4.9 mM range of values previously reported for hCBS (Kraus *et al.*, 1978; 1994; 1998; Banerjee *et al.*, 1998; Janosik *et al.*, 2001; Kruger *et al.*, 2006; Frank *et al.*, 2007). The change in $K_m^{L\text{-}Hcys}$ and k_{cat} are likely due to modification of the kinetic model to include a term for the observed substrate inhibition by L-Hcys (Scheme 3.1) and relief of product inhibition by the continuous assay, respectively. Substrate inhibition has not been reported for the wild-type human enzyme, although yeast CBS is known to be similarly inhibited at elevated L-Hcys concentration (Jhee *et al.*, 2000). The ability of 6-His/hCBS to catalyze the reverse-physiological hydrolysis of L-Cth was also investigated (table 3.3) and the k_{cat} and $K_m^{L\text{-}Cth}$ values are 5-fold and 2-fold lower, respectively, than the corresponding values for the model yeast enzyme (Aitken and Kirsch, 2003). Similar to yeast CBS, the k_{cat} of the hCBS-catalyzed condensation reaction is 72-fold greater than that of the hydrolysis reaction.

In summary, the 6-His/hCBS construct provides a cost-effective and efficient expression system for purification and subsequent kinetic studies of wild type and mutants of hCBS. Characterization of 6-His/hCBS demonstrated that, similar to the yeast enzyme, hCBS is substrate inhibited by L-Hcys and has the ability to catalyze both the physiological reaction in which L-Ser and L-Hcys are condensed to form L-Cth and the reverse-physiological hydrolysis of L-Cth.

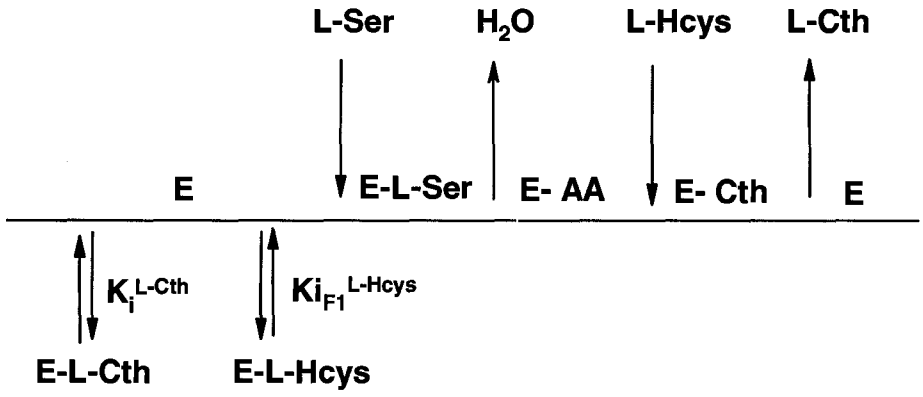

Scheme 3.1. Kinetic mechanism of hCBS, as modified to incorporate substrate inhibition by L-Hcys and possible product inhibition by L-Cth.

Chapter Four

The Effect of Over Expression and Mutation of Human Cystathionine β-Synthase on the Level of Glutathione in Mammalian Cells

4.1. INTRODUCTION

In mammals, transmethylation cycle and glutathione biosynthesis are linked by L-Hcys, the common precursor of the transmethylation and transulfuration pathways (Purdova *et al.,* 2006). It is suggested that more than 50% of the cell's cysteine is derived from homocysteine through this pathway (Banerjee *et al.,* 2000).

Glutathione (L-γ-glutamyl-L-cysteinyl-glycine), the major antioxidant of plant and animal cells, can attain millimolar concentrations in some cells. It exists in both reduced (GSH) and oxidized (GSSG) forms. The ratio [GSH]/[GSSG], which is often used as an indicator of the cellular redox state, is approximately ten under normal physiological conditions (Tietze 1969). This ratio is the major factor that determines the antioxidant capacity of cells and is maintained by GR. CBS catalyzes the rate-limiting step in the transulfuration pathway, thereby producing cysteine, the limiting precursor for glutathione synthesis. Banerjee *et al* (2000) observed that this pathway contributes up to 50% of the cysteine required for glutathione synthesis. However, CBS mutations can lead to accumulation of homocysteine, causing homocystinuria, and proposed to reduce the levels of cellular glutathione. More than 100 homocystinuria-associated point mutations of hCBS have been identified (http://www.uchsc.edu/cbs/cbsdata/mutations.htm). Five naturally occurring mutations hCBS (G305R, G307S, G148R, G259S and I278T) situated in proximity to the active site were selected to examine their effect on the activity of hCBS and on the level of glutathione. These mutants were created in hCBS, cloned into the mammalian expression vector pFLAG-CMV5 and transiently transfected into COS7 cells which have higher transfection efficiency. To understand the possible mechanism(s) by which these mutations affect the level of glutathione, attempts were made to express and

purify them *in vitro* using the bacterial expression vector pTrc99a (Chapter 3). Three of the five mutants could not be purified, likely due to improper folding and aggregation. Steady state kinetic studies, using the continuous assay developed by Aitken and Kirsch (2003), showed no detectable activity for G307S and weak activity for the G305R mutants *in vitro*. Mutants G148R, G307S, and I278T had large effects on total glutathione synthesis *in vivo*. Although the level of glutathione, as measured by the NADPH-recycling method of glutathione determination (Chapter 2), was increased by 35% upon over expression of wildtype CBS in COS7 cells, the site directed mutants did not significantly affect the total intracellular glutathione pool.

4.2. MATERIALS AND METHODS

4.2.1. Plasmid Construct for the *in vivo* Studies on hCBS

The plasmid selected for *in vivo* transient expression of hCBS in mammalian cells was pFLAG-CMV-5. Although the human embryonic kidney cell line HEK293, was employed here, future studies will use African green monkey COS7 embryonic kidney (American Type Culture Collection, Manassas, VA) that have very low levels of endogenously expressed hCBS. For ease of diagnosing the transfection and proper transient expression of the protein, a N-terminal FLAG-sequence (Asp-Tyr-Lys-Asp-Asp-Asp-Asp-Lys) was introduced into the hCBS sequence in the forward primer during PCR amplification. The hCBS gene was amplified using the hCBS-Fc-*EcoR*I forward primer: 5'-CCG AAT TC **ATG GAC TAC AAG GAC GAC GAT GAC AAA** CAT ATG CC-3' (FLAG DNA sequence in bold and underline) and an hCBS-Rc-*Sal*I reverse primer: 5'-GGA TCC GAT CGA CTT CAC TTC TGG TCC CGC-3'. The correct ligation of hCBS into the vector was verified by restriction digestion, PCR and sequencing. Expression of FLAG-hCBS was verified by transient transfection of pFLAG-CMV-5 containing hCBS and Western blotting with anti-FLAG-HRP. Transient transfections were carried out using Lipofectamine™ 2000 according to the manufacturer's protocol (Invitrogen, Carlsbad, CA).

4.2.2. Site Directed Mutagenesis

4.2.2.1. *In vitro* Mutant hCBS Expression Constructs

The overlap-extension method, described by Higuchi (Higuchi 1990) and the high-fidelity *pfu* (*Pseudomonas fluorescens*) DNA polymerase were employed for the production of all of the site-directed mutants of hCBS. The template was the bacterial expression plasmid pTrc99a containing the full-length sequence for wild type human CBS (hCBS) with an N-terminal, 6-His tag. The 5' and 3' ends of the insert, when amplified with forward pSECseq0 and reverse hCBS-Rc-*Sal*I primers, had *Nco*I and *Sal*I sites respectively and were ligated to the corresponding restriction endonuclease sites within the multiple cloning site of pTrc99a. The authenticity of all constructs was verified by DNA sequencing as well as PCR and restriction digests. The primers used for mutagenesis are listed in Table 4.1.

4.2.2.2. *In vivo* Mutant hCBS Expression Constructs

The overlap-extension protocol described in section 4.2.2.1 was utilized to construct the G148R mutant in the pFLAG-CMV-5 vector for *in vivo* expression, although the 5' and 3' flanking primers contained *EcoR*I and *Sal*I sites respectively. However, the remaining four hCBS mutants in the mammalian expression construct (G307S, G305R, G259S and I278T) were created by sub cloning from the pTrc99a mutants of hCBS into the unique *XmaI*/*Kas*I restriction endonuclease sites in the pFLAG-CMV-5/hCBS construct. All constructs was verified by DNA sequencing as well as PCR and restriction digests.

Table 4.1. Sequences of primers used in the construction of site-directed mutants of hCBS.

Oligo name	**Sequence 5' → 3'**
hFCBSG307Sf	GGTGGAAGGGATCTCGTACGACTTCATCCCC
hFCBSG307Sr	GGGGATGAAGTCGTACGAGATCCCTTCCACC
hFCBSG305Rf	ACCTACGAGGTGGAACGCATCGGCTACGACT
hFCBSG305Rr	AGTCGTAGCCGATGCGTTCCACCTCGTAGGT
hFCBSG148Rf	GCCGACATCCCGCAACACCGGGATCGGGC
hFCBSG148Rr	GCCCGATCCCGGTGTTGCGGGATGTCGGC
hFCBSG259Sf	CAGTGGGCACGGGCTCGACCATCACGGGC
hFCBSG259Sr	GCCCGTGATGGTCGAGCCCGTGCCCACTG
hFCBSI278Tf	CCTGGATGCAGGATCACCGGGGTGGATCCC
hFCBSI278Tr	GGGATCCACCCCGGTGATCCTGCATCCAGG

4.2.3. Transient Transfections of COS7 Cells and hCBS Expression

Transient transfections of pFLAG-CMV-5/hCBS expression constructs (wildtype and site-directed mutants) into COS7 cells were done using Lipofectamine™ 2000 according to the manufacturer's protocol. The optimal concentration of DNA was found to be 1.6 μg of DNA/0.5 mL of COS7 cells at a density of 1.5 X 10^6 cells/mL. Transfections were performed in 60 mm plates over 36 hours at 37°C and 5% CO_2 in a humidified tissue culture incubator (Thermo Forma, Marietta, OH).

4.2.4. Measurement of Intracellular Glutathione

Cells were harvested by cell lifting with subsequent washing with phosphate buffer saline (PBS) and centrifuged at 5,000 g for 5 minutes. Cells were lysed 1:5 (w/v) in ice-cold 5% sulfosalicylic acid (SSA; previously bubbled with nitrogen gas for 10 minutes), then bubbled with nitrogen gas for 10 seconds and centrifuged at 16,000 g in an Eppendorf microcentrifuge for 5 minutes. The supernatant was collected for GSH and GSSG analysis using the new method of NADPH recycling using G6PDH coupled to GR (Chapter 2).

4.2.5. Western Blotting

Following 36 hours of incubation at 37°C, transfected and untransfected (negative control) cells, were lysed using a cell lysis buffer (20 mM HEPES (pH 7.9), 420 mM NaCl, 1.5 mM $MgCl_2$, 0.2mM EDTA, and 25% glycerol) and total protein determined by using the Bradford reagent (Bio-Rad, Hercules, CA) with Bovine Serum Albumin (BSA) as a standard. Western blotting was performed using an anti-hCBS primary antibody (a gift from Dr. Warren D. Kruger) followed by HRP-conjugated anti-rabbit IgG secondary

antibody to diagnose transient expression of wildtype and site-directed mutants of hCBS in COS7 cells. Proteins were transferred from polyacrylamide gels to Immobilon-P transfer membranes (Millipore, Bedford, MA) at 180 mA and 4°C in a transfer buffer comprised of 20 mM Tris-HCl (pH 8.0), 150 mM glycine and 20% methanol. Following transfer, the membrane was blocked with 5% w/v non-fat dry milk in TBST buffer (20 mM Tris-HCl, pH 7.6, 137 mM NaCl and 0.1% Tween 20) for 1 hour prior to the primary antibody (1:10,000 dilution in blocking solution) and incubating for one hour at room temperature. The unbound antibody was removed by washing the blot for 3 X 30 minutes with TBST buffer at room temperature. The blot was then incubated for another 1 hour with the HRP-conjugated anti-rabbit IgG secondary antibody. Subsequently, it was washed for 3 X 30 minutes to remove the unbound secondary antibody. The blot was then incubated for one minute in 2 mL of the Renaissance chemiluminescence substrate (NEN Life Science Products, Boston, MA). The western blot was developed using autoradiography and then scanned with a Canoscan LiDE 80 desktop scanner.

4.2.6. Enzyme Assay for Mutants of hCBS

The continuous assay developed by Aitken and Kirsch (2003), described in Chapter 3 was used and data were fit to equation 3 and 4. However, the concentration range of the L-Hcys, and L-Ser substrates were varied depending on the kinetic parameters of the specific mutant to ensure that a range of substrate between approximately 0.1-20 fold of the K_m was employed.

4.3. RESULTS

The level of intracellular glutathione was measured after transient transfection COS7 cells with wild type and mutant hCBS in the pFLAG-CMV-5 expression vectors. The transfection efficiency of 3T3 cells was found to be less than that of the COS7 cells, there by necessitating a change of cell line. COS7 cells were selected because they have weak expression level of endogenous CBS and have high transfection efficiency. Previously, a mouse fibroblast (3T3) cell line, which has also undetectable level of endogenous CBS, was tested for this experiment. However, no strong difference between transfected and untransfected treatments was observed. The expression of the mutants was verified by western blot using anti-hCBS primary antibody followed by HRP-conjugated anti-rabbit IgG secondary antibody. Cell lysis with 5% sulfosalicylic acid precipitates all proteins in solution, thereby avoiding interference from protein thiol groups in the glutathione assay. The post-lysis pellet was resuspended in 0.5 M potassium phosphate buffer, pH 7.8 and used for total protein determination using the Bradford reagent (Bio-Rad protein assay reagent, Hercules, CA).

To understand the possible mechanism(s) by which naturally occurring mutations of human CBS affect levels of glutathione within the cell, an attempt was made to express and purify mutant CBS enzymes in *E. coli* with subsequent kinetic characterization.

Table 4.2. The steady state kinetic parameters of wildtype and G305R mutant hCBS.

Kinetic Parameters[a]	Wildtype	G305R mutant
k_{cat} (s^{-1})	2.7 ± 0.1	0.09 ± 0.01
$K_m^{L\text{-}Ser}$ (mM)	2.6 ± 0.3	0.6 ± 0.4
$K_m^{L\text{-}Hcys}$ (mM)	0.66 ± 0.06	0.04 ± 0.03
$k_{cat}^{L\text{-}Hcys} / K_m^{L\text{-}Hcys}$ ($mM^{-1}. s^{-1}$)	4.1 ± 0.1	2.1 ± 1.5
$k_{cat}^{L\text{-}Ser} / K_m^{L\text{-}Ser}$ ($mM^{-1}. s^{-1}$)	1.0 ± 0.1	0.2 ± 0.1
$K_{iF}^{L\text{-}Hcys}$ (mM)	7.2 ± 1.6	0.2 ± 0.2

[a]The kinetic parameters are obtained by using the continuous assay developed by Aitken and Kirsch (2003) as described in Chapter 2.

However, only two (G307S and G305R) of the five site-directed mutants could be purified. The remaining three (G148R, G259S and I278T) could not be purified, likely due to protein aggregation due to mis-folding resulting from the mutation (as observed from denaturing gels). The coupled-coupled continuous assay (Chapter 2) was used to characterize both G307S and G305R mutants (Table 4.2). There was no measurable activity for the G307S mutant.

4.3.1. pFLAG-CMV-5/hCBS construct

The correct ligation of the hCBS gene into the pFLAG-CMV-5 vector was verified by PCR using hCBS-Fc-*EcoR*I forward and hCBS-Rc-*Sal*I reverse primers (Figure 4.1A) and restriction digestion with *EcoR*I and *Sal*I (Figure 4.1B). Sequencing of the construct provided final confirmation of correct insertion as well as a lack of other mutations or frame shifts.

Upon transfection of the wild type and mutants of CBS, the COS7 cell lines showed a noticeable morphological change during the 36 hours of incubation. This change can be considered as a hallmark of the process of transfection. The transfected and control cells were harvested by cell lifting, washed with 1x PBS and lysed using N_2-bubbled cold 5% SSA for glutathione determination (Chapter 2). Thirty micrograms of total protein was run on a 10% SDS poly acrylamide gel and blotted using an anti-hCBS primary antibody, followed by HRP-conjugated anti-rabbit IgG secondary antibody (Figure 4.2) to visualize the expression level of CBS.

Figure 4.1. (A). Diagnostic PCR for the verification of ligation of N-terminal FLAG tagged hCBS into the *EcoRI*/*Sal*I site of the vector. **Lanes 1, 2, 3, 4** are different clones tested for the insert ligation; and **Lane M** is 1 Kb DNA ladder (New England BioLabs. Only two of the clones (Lanes 2 and 4) showed PCR product of the expected size. **(B).** *EcoRI*/*Sal*I digest pFLAG-CMV-5/hCBS expression construct. **Lanes 1, 2, 3, 4** are the different clones tested for the insert ligation and; **Lane M** is 1 Kb standard DNA ladder.

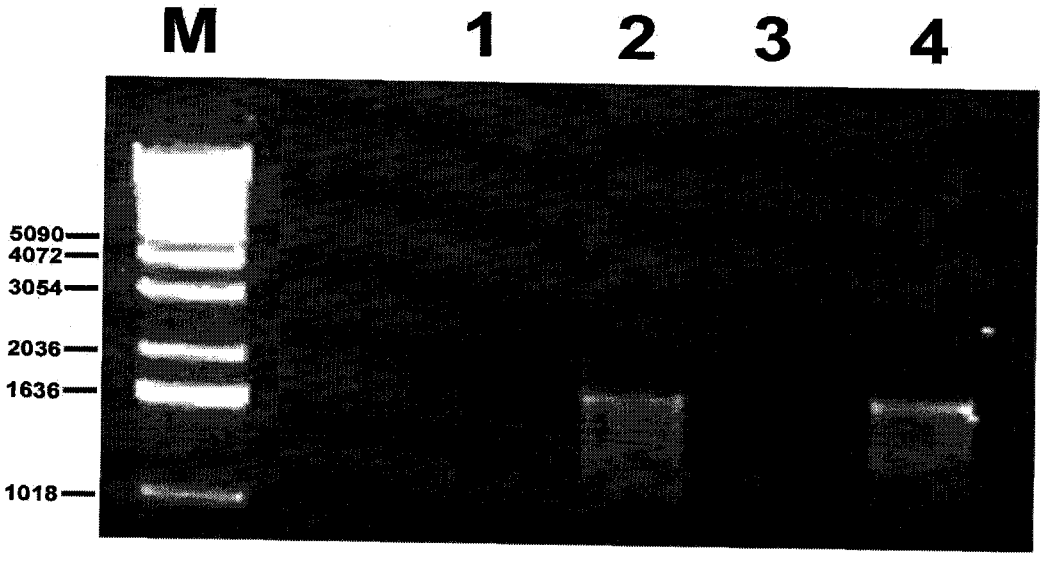
M
1
2
3
4
5090
4072
3054
2036
1636
1018

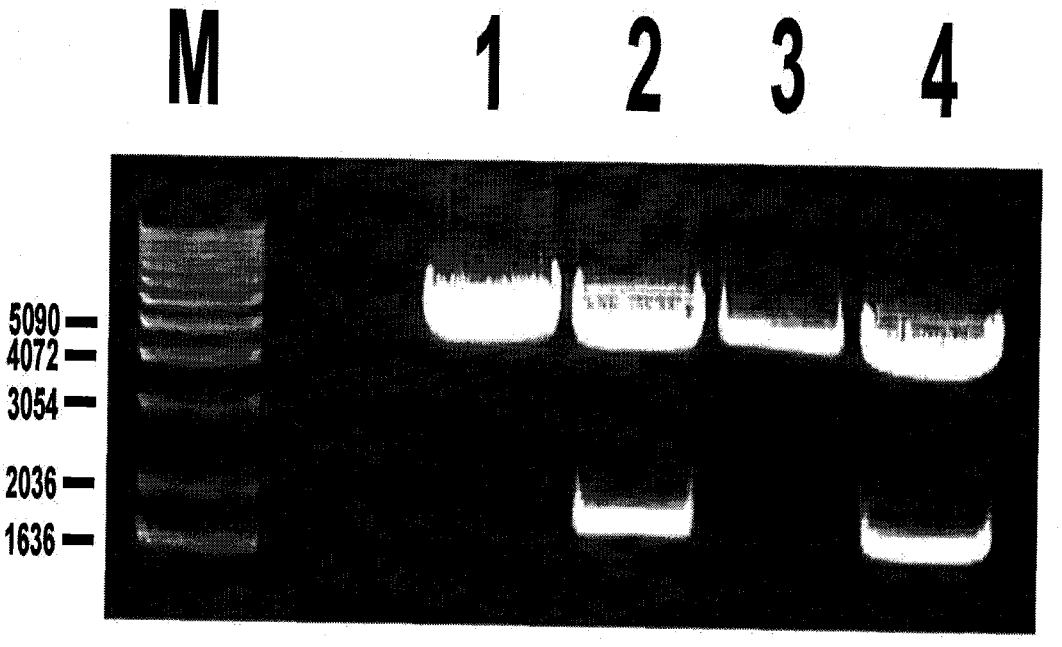
M
1
2
3
4
5090
4072
3054
2036
1636

Figure 4.2. Western blot of wild type and site-directed mutants of N-terminally FLAG-tagged human CBS expressed in COS7 cells. An anti-hCBS primary antibody, followed by HRP-conjugated anti-rabbit IgG secondary antibody, was used in the Western blot. **Lanes 1:** untransfected cell lysate; **2:** wildtype FLAG-hCBS; **3:** G307S mutant; **4:** G305R mutant; **5:** G148R mutant; **6:** G259S mutant; **7:** I278T mutant and **8:** 6x-His/hCBS (positive control). Right arrow indicates the correct molecular weight of hCBS (approximately 63 kDa).

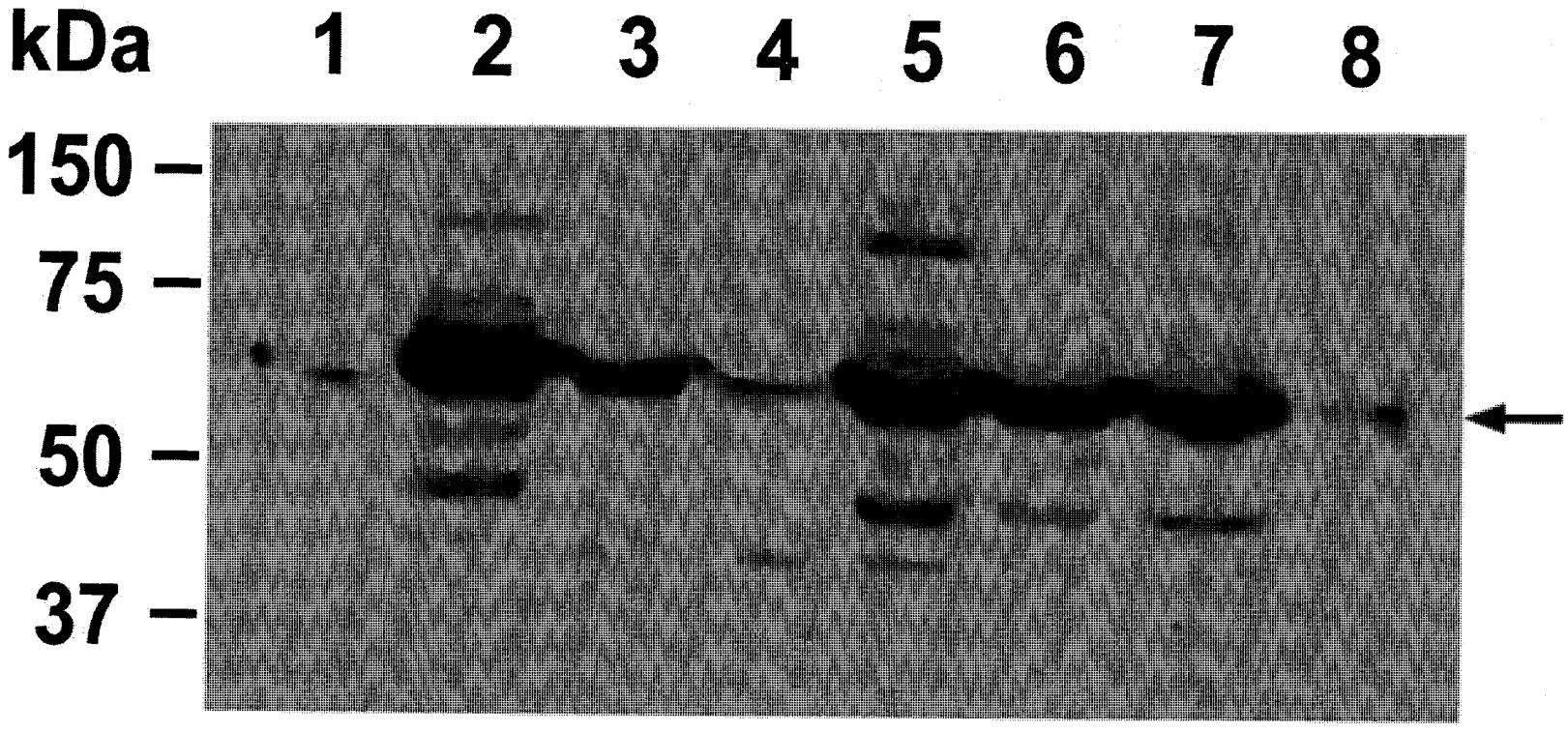
kDa
1
2
3
4
5
6
7
8
150
75
50
37

The effect of over expression of the wild type and mutants of CBS on the level of total and oxidized glutathione (Figure 4.3) was measured using GR-G6PDH recycling assay (Chapter 2). The level of GSSG or GSSG: GSH ratio is an indicator of the cellular oxidative status. Therefore, the observation that the GSSG or GSSG/GSH level of transfected cells was greater than the control (untransfected) cells (Figure 4.3) was not unexpected, as cells change their morphology upon transfection, due to oxidative stress caused either by either the process of transfection or to protein aggregation, for insoluble mutants. The lack of any statistically significant increment in the level of total glutathione for the mutants was either due to protein aggregation (G259S, G148R and I278T) or lack of activity (G305R and G307S) as observed *in vitro*. The extra protein bands for the wild type and mutants of hCBS out 63 kDa in the western blot (Figure 4.2) might be result of either multimerization (for the higher molecular weight bands) or partially degradation of the over expressed hCBS.

To confirm that changes in total glutathione were the result of the increased L-Cys production due to the transient expression of hCBS, as opposed to GR-mediated recycling of glutathione, COS7 cells transfected with wild type CBS were concomitantly exposed to varying concentrations of BSO (Figure 4.4). BSO is an inhibitor of γ-gluatmyl cysteine synthase, the enzyme which catalyzes the first step in glutathione biosynthesis. The level of glutathione showed nearly 90% decrease upon treatments with BSO.

Figure 4.3. (A). Total glutathione (GSH + GSSG) measured from COS7 cells after transfection with wildtype and site-directed mutants of hCBS. Glutathione determination was made from cell lysates made in 5% SSA. * indicates significant difference ($p<0.05$) from all others showing the effect of hCBS over expression (comparing with empty vector); ** indicates significant difference ($p<0.05$) from all others showing the effect of transfection (comparing with un transfected); *** indicating significant difference ($p<0.05$) from all others which might be speculated due to protein degradation of this mutant and subsequent cell death (comparing this mutant with all others). **(B).** Oxidized glutathione (GSSG) measured from COS7 cells after transient transfections with wild type and site-directed mutants of hCBS. GSSG determination was performed after derivatization of cell lysates with 0.5 M of 2-vinylpyridine for one hour at room temperature. ** shows significant difference from all others indicating that the process of transfection can cause oxidative stress. **(C).** GSSG/GSH ratio calculated after finding out the concentration of GSH by subtracting GSSG from total glutathione. ** shows significant difference ($p<0.05$) from all others showing the effect of transfection affecting the GSSG: GSH ratio. In all of the three graphs error bars are calculated as ± S.E.M from three independent transfections for total glutathione and sub replication for oxidized glutathione determinations.

A

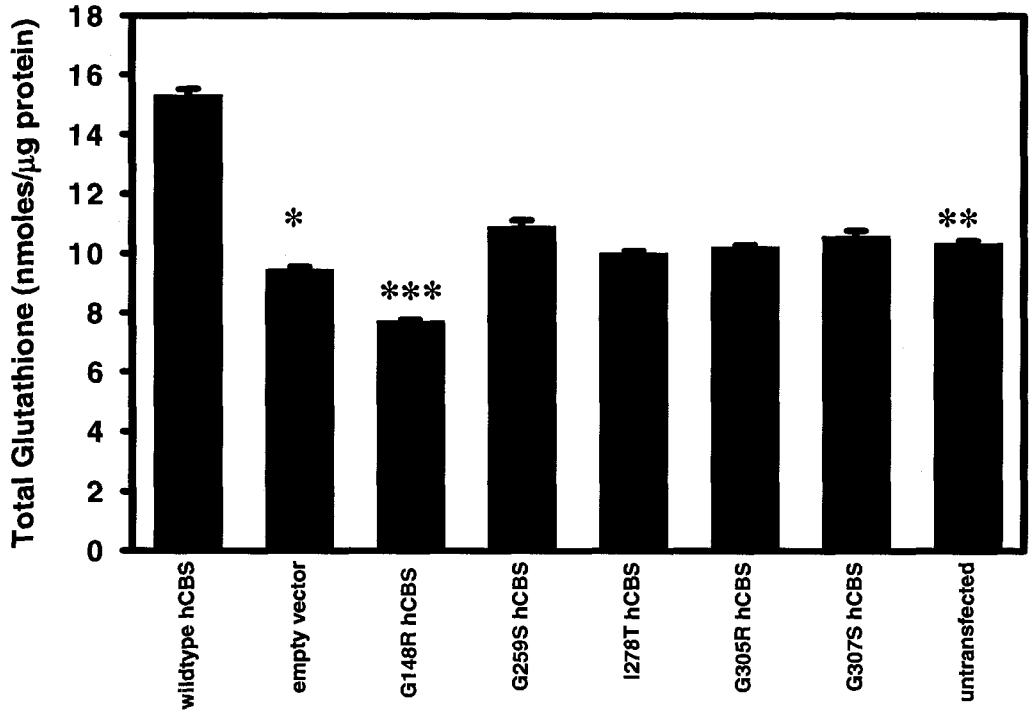
Total Glutathione (nmoles/µg protein)
18
16
14
12
10
8
6
4
2
0
*
***
**
wildtype hCBS
empty vector
G148R hCBS
G259S hCBS
I278T hCBS
G305R hCBS
G307S hCBS
untransfected

B

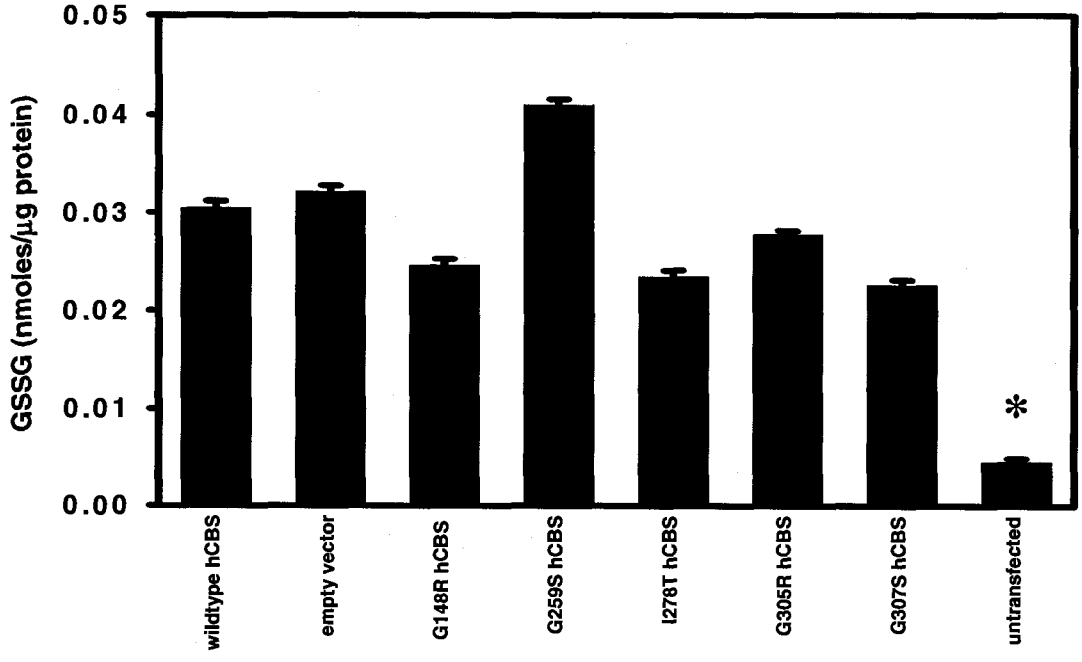
GSSG (nmoles/µg protein)
0.05
0.04
0.03
0.02
0.01
0.00
*
wildtype hCBS
empty vector
G148R hCBS
G259S hCBS
I278T hCBS
G305R hCBS
G307S hCBS
untransfected

C

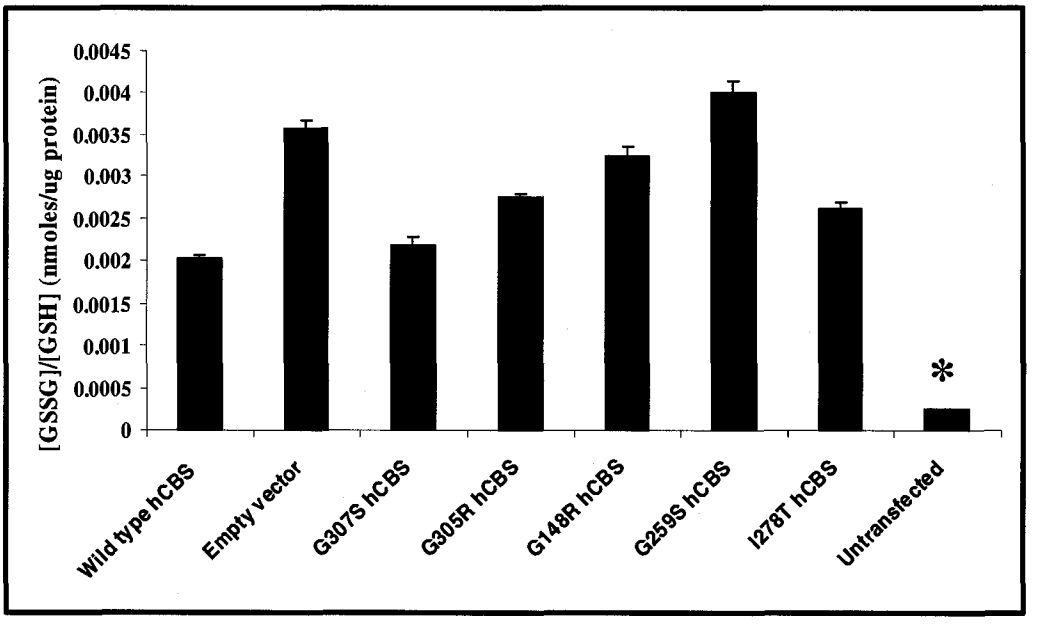
[GSSG]/[GSH] (nmoles/ug protein)
0.0045
0.004
0.0035
0.003
0.0025
0.002
0.0015
0.001
0.0005
0
*
Wild type hCBS
Empty vector
G307S hCBS
G305R hCBS
G148R hCBS
G259S hCBS
I278T hCBS
Untransfected

Figure 4.4. Total glutathione (GSH + GSSG) measured after transfection of COS7 cells with wildtype hCBS and concomitant treatment with varying concentrations of BSO: 0, 0.02, 0.10 and 0.2 mM.

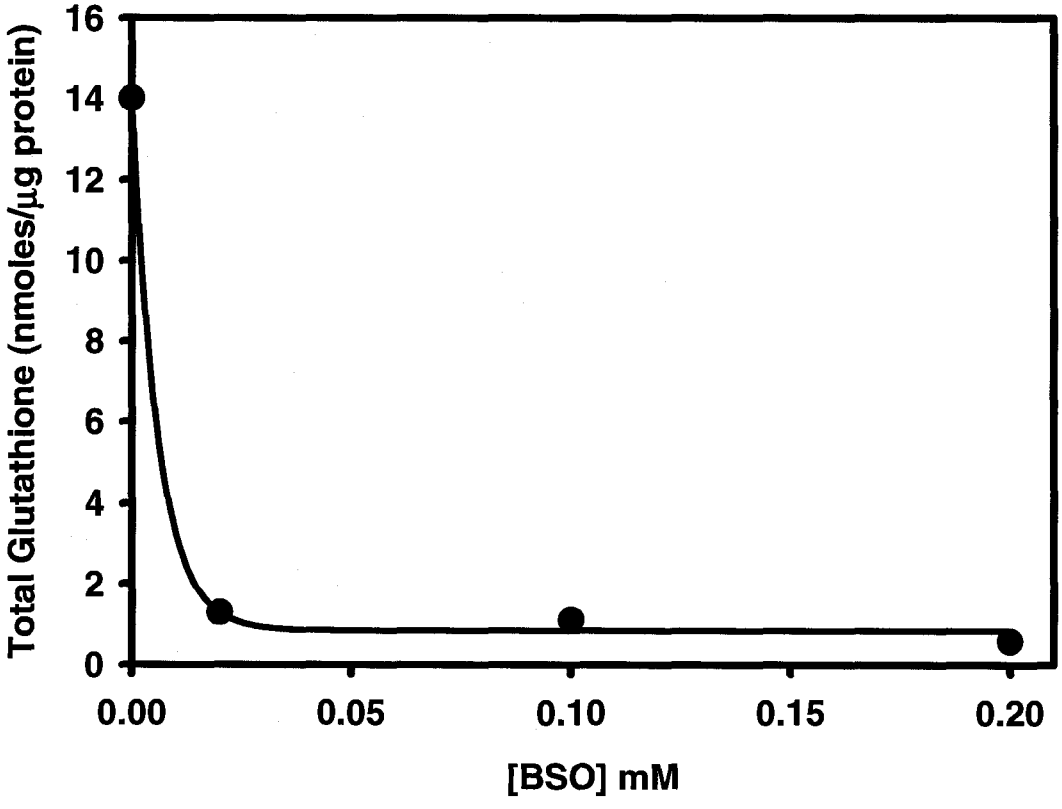
Total Glutathione (nmoles/µg protein)
16
14
12
10
8
6
4
2
0
0.00
0.05
0.10
0.15
0.20
[BSO] mM

4.4. DISCUSSION

The link between cellular methylation cycle and glutathione biosynthesis in mammalian cells is L-Hcys, a product of the methylation cycle. The two enzymes of the transulfuration pathway, CBS and CGL, catalyze the conversion of L-Hcys to L-Cys. The Latter is the limiting reagent in glutathione biosynthesis. Banerjee *et al* (2000) showed that 50% percent of the L-Cys required for glutathione biosynthesis is derived from L-Hcys.

As hCBS catalyzes the first step in the transulfuration pathway, mutations that reduce the catalytic efficiency of this enzyme lead not only to the accumulation of L-Hcys (and hence homocystinuria) but also to proposed declines in the levels of glutathione in cells. More than one hundred homocystinuria-associated point mutations have been identified in hCBS (http://www.uchsc.edu/cbs/cbsdata/mutations.htm N-terminally FLAG-tagged hCBS was transiently over expressed in COS7 cells to determine the effect of wild type enzyme and selected site-directed mutants (G148R, G259S, I278T, G305R, and G307S) on the intracellular concentration of glutathione. The G148R, G259S, G305R and G307S mutations are situated in proximity to the hCBS active site and were expected to have a profound effect on the catalytic efficiency of the enzyme and residue I278T is proposed to be involved in dimer interaction (Meier *et al.,* 2001). The level of glutathione increased by as much as 35% upon over expression of wild type hCBS. The direct effect of this over expression of the enzyme was confirmed by concomitant treatment of transfectants with varying concentrations of BSO (Figure 4.4) which inhibits γ-glutamyl cysteine synthase, the first enzyme in glutathione biosynthesis. The results showed that upon BSO treatments cells showed nearly 90% decrease in total intracellular glutathione level. Nevertheless,

over expression of the site-directed mutants did not affect (G307S) or show statistically insignificant increment of intracellular levels of glutathione (G259S, I278T and G305R).

The results (Figure 4.3B) showed that transfection may result in oxidative stress. Upon transfection, COS7 cells showed a dramatic increase (approximately 90%) in the levels of GSSG when compared to untransfected cells (negative controls). Interestingly, *in vitro* expression of G259S, I278T and G148R mutants showed protein aggregation likely due to mis-folding. This might suggest that the same phenomenon could be happening *in vivo* and probably inducing severe oxidative stress in addition to affecting the level of total intracellular glutathione.

Purification of the five site-directed hCBS mutants was attempted using the bacterial expression construct (pTrc99a/6-His/hCBS) described in Chapter 2. However, as the G148R, G259S and I278T mutants are insoluble, only the G307S and G305R enzymes were successfully purified. No measurable activity was observed for G307S and the k_{cat} of the G305R mutant was reduced by 30-fold (Table 4.2), suggesting that these mutants have insufficient activity to alter the cellular glutathione concentration *in vivo*.

In summary, over expression of hCBS in a cell line with undetectable endogenous levels of CBS can be used as a starting model to understand the effect of homocystinuria-related mutants of CBS on the levels of glutathione and the antioxidant status of the cell in general.

The model will further our understanding of the metabolic link between the transulfuration and glutathione biosynthesis pathways with respect to the effects of natural defects on the rate-limiting enzyme in the former pathway, CBS, on the production of the final metabolite of the later pathway, glutathione.

In addition, this model reveals that homocystininuria-associated mutations of CBS not only affect the levels of homocysteine in patients but also may affect their antioxidant defences against prooxidant stresses.

5. CONCLUSION

Human cystathionine β-synthase catalyzes the committing step in the transulfuration path way which converts L-Hcy to L-Cys, a precursor of gluatathione biosynthesis. This path way is responsible for 50% of the cysteine (Banerjee *et al.,* 2000) required for *de novo* synthesis of glutathione. Homocystinuria-associated point mutations of hCBS, leading to the dysfunctional forms of the enzyme, may affect the glutathione concentration of mammalian cells, thereby reducing their antioxidant capacity. This study examined the effect of transiently expressing point mutants of hCBS on the cellular concentration of glutathione in mammalian cells. Essential first steps to enable this work were the refinement and assessment of a glutathione quantification assay and the development of bacterial and mammalian expression system.

The conventional glutathione assay, developed by Tietze (1969) and modified by Griffith (1980), utilizes GR to reduce GSSG and make it available for an uncatalyzed reaction with DTNB (Scheme 2.1). Recently (Neumann *et al.,* 2003), an enzymatic method has been developed which recycles the nicotinamide adenine dinucleotide phosphate (NADPH) cofactor required by GR. This method couples glucose-6-phosphate dehydrogenase (G6PDH) with GR, thereby allowing the continuous regeneration of the limiting reagent NADPH from $NADP^+$ (Scheme 2.2). The present study refines the method of Neumann *et al.* (2003) by optimizing the conditions in order to minimize G6PDH and G6P usage, thereby reducing its cost to make it more amenable as a high throughput technique. The accuracy and detection limit of this assay was compared with the standard GR-based assay (Scheme 3.1) as well as HPLC coupled with electrochemical detection; the method currently considered to be the most sensitive (Kruusma *et al.,* 2006). The

NADPH-recycling recycling assay is more accurate at measuring total and reduced glutathione but may have a similar accuracy for oxidized glutathione. Differences in detection limits of GSH and GSSG in whole cell lysates between recycling and conventional assays were reflected in differences in the standard curves between the two methods. In general, the NADPH-recycling method detected two- to thirteen-fold more GSH in cell lysates than the conventional method. BSO is inhibitor of γ-glutamylcysteine synthase, the enzyme that catalyzes the first and rate-limiting step of glutathione biosynthesis pathway; the linkage of cysteine and glutamate. Levels of glutathione were measured after treatment of HEK 293 cells with BSO. The recycling method measured 1.2- to 13.5-fold more total glutathione in untreated cells than the conventional method, due to the higher upper limit of the NADPH-recycling assay

The steady state kinetic characterization of hCBS requires the purification of sufficient (milligram quantities) of enzyme. However, the existing bacterial expression systems are expensive and laborious. Therefore, expression constructs were designed that include a 6-His tag to enable the use of metal ion affinity chromatography, using Ni-NTA resine. The three expression constructs tested were 6-His-GST/hCBS, 6-His/GFP/hCBS and 6-His-hCBS. The yield and steady state kinetic parameters of hCBS expressed using the three different constructs were compared and 6-His/hCBS was found to be optimal. Purification of 6-His-GST/hCBS and 6-His-GFP/hCBS *via* Ni-NTA chromatography yielded protein of only approximately 50% (Figure 3.3A) and >80% (Figure 3.4A) purity, respectively. Thrombin treatment of the GST and GFP fusion proteins was successful as the expected 26 (GST) and 27 (GFP) and 63 kDa (hCBS) bands were observed, while the 90- kDa band of the fusion protein was not observed following successful cleavage

(Figures 3.3B and 3.4B). In contrast, the 6-His/hCBS was >90% pure, did not require protease cleavage and yielded ~5-fold more protein than the GST and GFP fusion constructs. The activity of the hCBS enzyme produced with each of the three expression constructs was assayed using the continuous CBS assay (Aitken and Kirsch, 2003). Comparison of the kinetic parameters (Table 3.2) demonstrates that the $K_{cat}/K_m^{L\text{-}Hcys}$ and $K_{cat}/K_m^{L\text{-}Ser}$ of 6-His/hCBS were increased 8- and 13-fold, compared to for hCBS from the GST and GFP constructs, respectively. The steady state kinetic parameters of 6-His/hCBS were fully characterized over a wider range of concentrations of L-Ser and L-Hcys. The data were fit to equation 4. Such global fit revealed for the first time a new steady state kinetic parameter of substrate inhibition by L-Hcys (Table 4.2).

The model system developed for the study of the effect of naturally occurring missense mutations of hCBS on the level of glutathione showed a clear difference between wild type and select mutants upon transfections of COS7 cells. Transfection of wildtype hCBS resulted in nearly 35% increment in the level of total glutathione. This level of glutathione was taken as a point of reference to examine the effect of selected naturally occurring point mutations of hCBS. Remarkably, the level of total glutathione upon transfection of these mutants showed no difference from the negative control. Verification of the involvement of over expression of hCBS on the transulfuration pathway was analyzed by using varying concentration of BSO, inhibitor of γ- gluatmyl synthase.

Future directions may focus on testing the ability of cells to protect them selves against prooxidant stress if they have CBS mutations. Gene "knock in" of CBS mutants could create stable cell lines that continuously express these mutants. Gene knock down of hCBS may also affect the levels of glutathione as well as the cells ability to protect itself against prooxidant stress. This opens up the possibility for future studies involving *in vitro* manipulation of CBS in cell lines and the effects of a variety of oxidative stressors on glutathione synthesis and cell viability.

6. REFERENCES

Aitken, S.M. and Kirsch, J.F. (2003). Kinetics of the yeast cystathionine ß-synthase forward and reverse reactions: continuous assays and the equilibrium constant for the reaction. Biochemsitry 42:571-578

Anderson, M.E. (1998). Glutathione: an overview of biosynthesis and modulation. Chemico-biol. Interact. 111-112: 1-14

Banerjee, R., and Kabil, O. (1999). Deletion of the regulatory domain in the pyridoxal phosphate-dependent heme protein cystathionine β-synthase alleviates the defect observed in a catalytic site mutant. J. Biol. Chem. 274:31256-31260

Banerjee, R., Mosharov, E., and Cranford, M.R. (2000).The qantitatively important relationship between homocysteine metabolism and glutathione synthesis by the transsulfuration pathway and its regulation by redox changes. Biochemistry 39:13005-13011

Banerjee, R., Taoka, S., Ohja, S., Shan, X. and Kruger, W.D. (1998). Evidence for heme-mediated redox regulation of human cystathionine β-synthase activity. J. Biol Chem. 273: 25179-25184

Bousquet, E., Santagati, N.A. and Lancetta, T. (1989). Determination of glutathione in biological tissues by high performance liquid chromatography with electrochemical detection. J. Pharm. Biomed. Anal. 7: 643-647

Burstyn, J.N., Kraus, J.P., Rodgers, K.R., Clark, R.W., Park, R.B., Rees, K.A., Oliveriusovai, J., Lukat-Rodegers, Gudrun, S. and Pazieni, S. (2004). The redox behavior of the heme in cystathionine β-synthase is sensitive to pH. Biochemistry 43:14684-14695

Bukhard, P., Tai, C.H., Ristroph, C.M., Cook, P.F. and Jansonius, J.N. (1999). Ligand binding induces a large conformational change in o-acetylserine sulfhydrylase from *Salmonella typhimurium*. J. Mol. Biol. 291: 941-953

Chalfie, M. and Kain, S. (Eds). In: Green fluorescent protein: properties, applications, and protocols. New York: Wiley-Liss. (1998). pp 77-96

Chen, Z., Crippen, K., Gulati, S. and Banerjee, R. (1994). Purification and kinetic mechanism of mammalian methionine synthase from pig liver. J. Biol. Chem. 44: 27193-27197

Clarke, R., Smith, A.D., Jobst, K.A., Retsum, H., Sutton, L. and Ueland, P.M. (1998). Folate, vitamin B_{12}, and serum total homocysteine levels in confirmed Alzheimer disease. Arch. Neurol. 55:1449-1455.

Chalfie, M., Tu, Y., Euskirchen, G., Ward, W.W., and Prasher, D.C. (1994). Green fluorescent protein as a marker for gene expression. Science 263:802-805

Elliott, A.J., Scheiber, S.A, Thomas, C. and Pardini, R.S. (1992). Inhibition of glutathione reductase by flavonoids: a structure-activity study. Biochem. Pharmacol. 44, 1603–8.

Ellman G.L. (1959). Tissue sulfhydryl groups, Arch. Biochem. Biophys. 82: 70-77.

Fang, Y.Z, Yang, S. and Wu, G. (2002). Free radicals, antioxidants, and nutrition. Nutrition 18:872-879.

Frank, N., Kent, J.O., Meier, M. and Kraus J.P. (2007). Purification and characterization of the wild type and truncated human cystathionine β-synthase enzymes expressed in *E. coli*. Arch. Biochem. and Biophys. doi:10.1016/j.abb.2007.11.006

Finkelstein, J.D. (1990). Methionine metabolism in mammals. J. Nutr. Biochem. 1: 228-237

Finkelstein, J.D. and Martin, J.J. (1984). Methionine metabolism in mammals. Distribution of homocysteine between competing pathways. J. Biol. Chem. 15: 9508 - 9513

Galas, D.J., Hemsley, A., Arnheim, N., Toney, M.D. and Cortopassi, G. (1989). A simple method for site-directed mutagenesis using the polymerase chain reaction. Nucleic Acids Res. 25: 6545–6551

Giustarini, D. Dalle-Donne, I., Colombo, R., Milzani, A. and Rossi, R. (2003). An improved HPLC measurement for GSH and GSSG in human blood. Free Radic. Biol. Med. 35: 1365-1372.

Griffith, O.W. (1980). Determination of glutathione and glutathione disulfide using glutathione reductase and 2-vinylpyridine. Anal. Biochem. 106: 207-212.

Haddad, J.J.E, Oliver, R.E. and Land, S. (2000). Antioxidant/Pro-oxidant equilibrium regulates HIF-1α and NF-κB. J. Biol. Chem. 275: 21130-21139.

Harvey, P.R., Ilson, R.G. Strasberg, S.M. (1989). The simultaneous determination of oxidized and reduced glutathione in liver tissues by ion pairing reverse phase high performance liquid chromatography with a coulometric electrochemical detector, Clin. Chem. Acta. 180: 203-212.

Harker, L.A, Slichter, S.J., Scott, C.R. and Ross, R. (1974). Homocystinemia, vascular injury and arterial thrombosis. N. Engl. J. Med. 291(11): 537-543

Higuchi, R. (1990). PCR protocols. Academic Press, San Diego, CA

http://www.uchsc.edu/cbs/cbsdata/mutations.htm

Hu, F.L., Gu, Z., Kozich, V., Kraus, J.P., Ramesh, V. and Shih, V.E. (1993). Molecular basis of cystathionine β-synthase deficiency in pyridoxine responsive and nonresponsive homocystinuira. Hum. Mol. Genet. (2) 11: 1857-1860

Janosik, M., Kery, V., Gaustadnes, M., Maclean, K.N. and Kraus, J.P. (2001). Regulation of human cystathionine β-synthase by s-adenosyl-l-methionine: evidence for two catalytically active conformations involving an autoinhibitory domain in the C-terminalrRegion. Biochemistry 35: 10625–10633

Jhee, K.H, McPhie, P. and Miles, E.W. (2000). Yeast cystathionine β-synthase is a pyridoxal phosphate enzyme but, unlike the human enzyme, is not a heme protein. J. Biol. Chem. 275: 11541-11544.

Jones, D.P. (2002). Redox potential of GSH/GSSG couple, assay and biological significance. Meth. Enzymol. 348: 93-112

Kaplowitz, N., Aw, T.Y. and Ookhtens, M. (1985). The regulation of hepatic glutathione, Annu. Rev. Pharmacol. Toxicol. 25: 715-744.

Kraus, J.P. (1994). Molecular basis of phenotype expression in homocystiniuria. J. Inher. Metab. Dis. 17:383-390

Kraus, J.P., Bukovska, G., and Kery, V. (1994). Expression of Human Cystathionine β-Synthase in *Escherichia coli*: Purification and Characterization. Protein Expr. Purif. 5: 442 – 448.

Kraus, J.P., Janosik, M., Kozich, V., Mandell, R., Shih, V., Sperandeo, M.P., Sebastio, G., de Franchis, R., Andria, G., Kluijtmans, L.A.J., Blom, H., Boers, G.H.J., Gordon, R. B., Kamoun, P., Tsai, M.Y., Kruger, W.D., Koch, H.G., Ohura, T., and Gaustadnes, M. (1999). Cystathionine β-synthase mutations in homocystinuria. Human Mutations. 13: 362 - 375

Kraus, J., Packman, P.S., Fowler, B., and Rosenberg, L.E. (1978). Purification and properties of cystathionine β-synthase from human liver. Evidence for identical subunits. J. Biol. Chem. 253: 6523 – 6528.

Kraus, J.P, and Rosenberg, L.E. (1983). Cystathionine β-synthase from human liver: Improved purification scheme and additional characterization of the enzyme in crude and pure form. Arch. Biochem. Biophys. 222: 44 – 52.

Kruger, W.D., Chen, X., Wang, L. and Fazlieva, R. (2006). Contrasting behaviours of mutant cystathionine β-synthase enzymes associated with pyridoxine response. Human Mutation 27: 474 - 482

Kruger, W.D., Liqun, W., Kwang-Hwan, J., Xiang, H., Patricia, M.D. and Donald, W.J. (2004). Modulation of cystathionine β-synthase level regulates total homocysteine in mice. American Heart Association 94: 1318 – 1324

Lakritz, J., Plopper, C.G. and Buckpitt, A.R. (1997). Validated high-performance liquid chromatography-electrochemical method for determination of glutathione and glutathione disulfide in small tissue samples. Anal. Biochem. 247: 63 - 68.

Lewicki, K., Marchand, S., Matoub, L., Lulek, J. Coulon, J. and Leroy, P. (2006). Development of a fluorescence-based microtitre plate method for the measurement of glutathione in yeast. Talanta 70: 876 - 882.

Lu, S.C. (2000). Regulation of glutathione synthesis. Curr. Topi. Cell. Regul. 36:95-116.

Maclean, K.N., Janošík, M., Oliveriusová, J., Kery, V., and Kraus, J.P. (2000). Transsulfuration in *Saccharomyces cerevisiae* is not dependent on heme: purification and characterization of recombinant yeast cystathionine β-synthase. J. Inorg. Biochem. 81: 161-171

Medina, M. A., Urdiales, J.L. and Amores-Sanchez, M.I. (2001). Roles of homocysteine in cell metabolism, old and new functions. Euro. J. Biochem. 268:3871-3882.

Mehta, P.K., and Christen, P. (2000). The molecular evolution of pyridoxal-5'-phosphate-dependent enzymes. Adv. Enzymol. Relat. Areas Mol. Biol. 74:129-133

Meier, M., Kery, V., Janosik, M., Kraus, J.P. and Burkhard, P. (2001). Structure of human cystathionine β - synthase:a unique pyridoxal 5'-phosphate-dependent heme protein. EMBO J. 20: 3910-3916.

Meier, M., Oliveriusora J., Kraus J.P. and Burkhard, P. (2003). Structural insights into mutations of cystathionine β-Synthase. Biochem. Biophys. Acta 1647: 206-213.

Mourad, T., Min, K.L., Steghens, J.P. (2000). Measurement of oxidized glutathione by enzymatic recycling coupled to bioluminescent detection. Anal. Biochem. 283 146-152.

Mudd, S.H., Dkovby, F., Levy, H.L., Pettigrew, K.D., Wilcken, B. and Pyeritz, R.E. (1985). The natural history of homocystinuria due to cystathionine β-synthase. Am. J. Hum. Genet. 37: 1-31

Neumann, C., Grunert, B.R. and Bednarski, P.J. (2003). Nicotinamide adenine dinucleotide phosphate-regenerating system coupled to a glutathione-reductase micro titer method for determination of total glutathione concentrations in adherent growing cancer cell line. Anal. Biochem. 320: 170-178

Nörgren, S., and Njalsson, R. (2005). Physiological and pathological aspects of GSH metabolism. Acta Pediatrica. 94:132-137

Nozaki, T., Shigeta, Y., Saito-Nakano, Y., Imada, M. and Kruger, W.D. (2001). Characterization of transsulfuration and cysteine biosynthetic pathways in the protozoan haemoflaggelate, *Trypanosoma cruzi*. Isolation and molecular characterization of cystathionine β-synthase and serine acetyltransferase from Trypanosoma. J. Biol. Chem. 276: 6516-6523

Ojha, S., Wu, J., LoBrotto, R. and Banerjee, R. (2002). Effects of heme ligand mutations including a pathogenic variant, H65R, on the properties of human cystathionine β-synthase. Biochemistry 41: 4649- 4654.

Oliveriusová, J., Kery, V., Maclean, K.N. and Kraus, J.P. (2002). Deletion mutagenesis of huamn cystathionine β-synthase: impact on activity, oligomeric status and s-adenoylmethionine regulation. J. Biol. Chem. 50: 48386 - 48394

Outinen, P.A., Sood, S..K., Liaw, P.C.Y., Sargg, K.D., Maeda, N., Kirsch, J., Ribau, J., Podor, T. J, Weitz J.I. and Austin, R.C. (1998). Characterization of the stress-inducing effects of homocysteine. Biochem. J. 332: 213- 221.

Poppenborg, L., Frieh, K. and Flaschel, E. (1997). The green fluorescent protein is a versatile reporter for bioprocess monitoring. J. Biotechnol. 58: 79 - 88

Purdova, A, Banerjee, R., Bauman, Z., Braun, A., Vitvitsky. V. and Lu, S.C. (2006). S-adenosylmethionine stabilizes cystathionine β-synthase and modulates redox capacity. Proc. Natl. Acad. Sci. USA. 103: 6489-6494

Reed, D.J., Babson, J.R., Beatty, P. W. Brodie, A.E., Ellis, W.W., and Potter, D.W. (1980). High-performance liquid chromatography analysis of nanomole levels of glutathione, glutathione disulfide and related thiols and disulfides. Anal. Biochem. 106: 55 - 62.

Reglinski, J., Smith, W.E., Brzeski, M., Marabani, M. and Sturrock, R.D. (1999). Clinical analysis by ^{1}H spin-echo NMR oxidation of intracellular glutathione as a consequence of penicillamine therapy in rheumatoid arthritis. J. Med. Chem. 35: 2134 - 2137.

Rellán-Álvarez, R., Hernández, L.E., Abadia, J. and Álvarez-Fernández, A. (2006). Direct and simultaneous determination of reduced and oxidized glutathione and homoglutathione by liquid chromatography-electrospray/mass spectrometry in plant tissue extracts. Anal. Biochem. 356: 254-264.

Serru, V.B., Baudin, F., Ziegler, J.P., David, M.J., Cals, M. and Vaubourdolle, N.M. (2001). Quantification of reduced and oxidized glutathione in whole blood samples using capilliary electrophoresis. Clin. Chem. 47: 1321-1324

Seiwert, B. and Karst U. (2007). Simultaneous LC/MS/MS determination of thiols and disulfides in urine samples based on differential labeling with ferrocene-based maleimides. Anal. Chem. 79: 7131- 7138

Shaik, I.H. and Mehvar, R. (2006). Rapid determination of reduced and oxidized glutathione levels using a new thiol-masking reagent and the enzymatic recycling method: application to the rat liver and bile samples. Anal. Bioanal. Chem. 385: 105-113

Shan, X., Dunbrack, R.L., Chritopher, S.A. and Kruger, W.D. (2001). Mutations in the regulatory domain of cystathionine β-synthase can functionally suppress patient-derived mutations *in cis*. Hum. Mol. Genet. 6: 635-643.

Shan, X., and Kruger, W.D. (1998). Correction of disease causing CBS mutations in yeast. Nat. Genet. 19:91-93.

Shike, M. (Ed.) (2006). Modern nutrition in health and disease. Lippincott, Williams and Wilkins. Philadelphia.

Sies, H. (1999). Glutathione and its role in cellular functions. Free Radic. Biol. Med. 27: 916-921.

Taoka. S., Widjaja. L., and Banerjee, R. (1999). Assignment of enzymatic functions to specific regions of the PLP-dependent hemeprotein cystathionine ß-synthase. Biochemistry 38: 13155- 13161

Teodoro, B. (2002). *S*- adenosyl-L-methionine (SAMe): from the bench to the bedside-molecular effects of a pleotrophic molecule. Am. J. Clin. Nut. 5: 1151S - 1157S

Tietze, F. (1969). Enzymatic method for quantitative determination of nanogram amounts of total and oxidized glutathione: applications to mammalian blood and other tissues. Anal. Biochem. 27: 502-522

Townsend, D.M., Tew, K.D., and Tapiero, H. (2003). The importance of glutathione in human disease. Biomed. Pharmacother. 57:145-155.

Vogel, H.,J., and Bonner, D.M. (1956). Acetylornithinase of *Escherichia coli*: partial purification and some properties. J. Biol. Chem. 218: 97–106

Wu, G., Fang, Y., Yang, S., Lupton, J.R. and Turner, N.D. (2004). Glutathione metabolism and its implication for Health. Rec. Adv. Nutrit. Sci. 0022-3166/04.

Yang, F., Larry G. Moss, and George N. Phillips, Jr. (1996). The Molecular basis of green fluorescent protein. Nature Biotechnology. 14: 1246-1251